university of groningen

University Medical Center Groningen

University of Groningen

Control of nanopore formation using external triggers

Mutter, Natalie

DOI:
10.33612/diss.131163011

IMPORTANT NOTE: You are advised to consult the publisher's version (publisher's PDF) if you wish to cite from it. Please check the document version below.

Document Version
Publisher's PDF, also known as Version of record

Publication date:
2020

Link to publication in University of Groningen/UMCG research database

Citation for published version (APA):
Mutter, N. (2020). *Control of nanopore formation using external triggers*. [Thesis fully internal (DIV), University of Groningen]. University of Groningen. https://doi.org/10.33612/diss.131163011

Copyright
Other than for strictly personal use, it is not permitted to download or to forward/distribute the text or part of it without the consent of the author(s) and/or copyright holder(s), unless the work is under an open content license (like Creative Commons).

The publication may also be distributed here under the terms of Article 25fa of the Dutch Copyright Act, indicated by the "Taverne" license. More information can be found on the University of Groningen website: https://www.rug.nl/library/open-access/self-archiving-pure/taverne-amendment.

Take-down policy
If you believe that this document breaches copyright please contact us providing details, and we will remove access to the work immediately and investigate your claim.

Downloaded from the University of Groningen/UMCG research database (Pure): http://www.rug.nl/research/portal. For technical reasons the number of authors shown on this cover page is limited to 10 maximum.

Download date: 05-05-2023

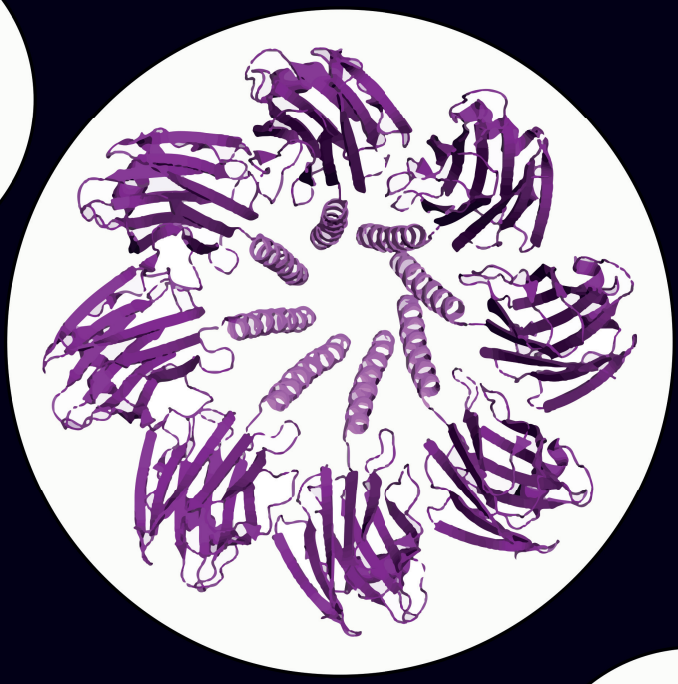

2

Modular pore-forming immunotoxins with caged cytotoxicity tailored by directed evolution

Natalie L. Mutter[1], Misha Soskine[1], Gang Huang[1], Inês S. Albuquerque[2], Gonçalo J. L. Bernardes[2,3] and Giovanni Maglia[1*]

[1]Groningen Biomolecular Science & Biotechnology Institute, University of Groningen, Nijenborg 4, 9747 AG, Groningen, Netherlands

[2]Instituto de Medicina Molecular, Faculdade de Medicina, Universidade de Lisboa, Avenida Professor Egas Moniz, 1649-028, Lisboa, Portugal

[3]Department of Chemistry, University of Cambridge, Lensfield Road, Cambridge CB2 1EW, UK

***ACS Chem. Biol.* 2018 Nov 16; 13 (11): 3153-3160.**

ABSTRACT

Immunotoxins are proteins containing a cell-targeting element linked to a toxin that are under investigation for next-generation cancer treatment. These agents, however, are difficult to synthesize, chemically heterogeneous, expensive and show toxicity toward healthy cells. In this work, we describe the synthesis and characterization of a new kind of immunotoxins that showed exquisite selectivity toward targeted cells. In our construct, targeting molecules were covalently attached or genetically fused to oligomeric pore-forming toxins. The activity of the immunotoxin was then caged by fusing a soluble protein to the transmembrane domain and activated via cleavage with furin, a protease overexpressed in many cancer cells. During the several coupling steps, directed evolution allowed to efficiently synthesize the molecules in *E. coli* cells, and to select for further specificity toward targeted cells. The final construct showed no off-target activity, while acquiring an additional degree of specificity toward the targeted cells upon activation. The pore-forming toxins described here do not require internalization to operate; while the many protomeric subunits can be individually modified to refine target specificity.

INTRODUCTION

Protein-based drugs have become increasingly important in the pharmaceutical industry. In the 2011–2016 period the FDA approved 62 proteins as drugs[1], most of which contain monoclonal antibodies (mAb). These agents recognize molecular targets on cancer cell surfaces, blocking their biological function, or, most often, marking the cells for the body's immune system.[2] An advantage of this approach is that drugs can be developed to recognize specifically a complex biological signature in malignant cells. However, mAbs are complex molecules that cannot be synthesized chemically and are manufactured in living organisms.[3] Further, they often require complex post-translational modifications that can only be introduced when heterologous expression systems are used.[4] Additionally, as the products are synthesized by cells or organisms, their chemical modification is not straightforward, and complex purification processes are involved.[5,6] Finally, because their large size (up to 150 kDa), they have limited tumor penetration[7], and they are often recognized by the host immune system.[8]

In next-generation targeted cancer therapy [9], mAbs were e.g. conjugated to a drug (antibody-drug conjugates)[1,10,11], to a toxin (immunotoxin or IT)[12,13], to a cytokine[14] or to a radioactive particle [15]. In such constructs, the antibody recognizes a specific cell target allowing the deadly cargo to be delivered to the diseased tissue. In immunotoxins mAbs or growth factors are either chemically or genetically fused to a potent protein toxin which inhibit protein synthesis, such as diphtheria toxin[16] or pseudomonas exotoxin A[17]. These are very efficient toxins because they act catalytically on their cytosolic targets, hence at very low concentrations. However, ITs require being internalized into the cell and not every target has a sufficient internalization rate, allowing sufficient accumulation of toxophore to effectively kill cancer cells.[18–20] Hence, a highly potent payload drugs must be used frequently, which in turn can produce life-threatening toxicities.[21] In fact, the high potency of the payload requires a highly selective expression of membrane targets in cancer cells compared to healthy cells[22], and the number of suitable targets may be limited to just a few dozen.[23]

Alternative hybrid molecules might be built from membrane-acting toxins, which assemble unregulated oligomeric pores in the membrane of targeted cells. Different hemolytic toxins from sea anemones, bacteria or humans[24–26], have been used to target different cell lines, including immature T lymphocytes[27], leukemic cells[26], breast cancer cells[28], lung cancer cells[29] or colon cancer cells[30]. Since hundreds of pores might be necessary to obtain a cytotoxic effect [31], pore-forming toxins are much less potent than intracellular toxins commonly used in ITs. Toxicity, however, may be complemented or regulated by using other drugs, which are preferably internalized into

the cells permeabilized by the pore-forming toxin.[32] In addition, each monomer of the pore could be fused to different targeting elements, which in turn should bring a higher level of control of the targetability of the drug. The main limitation of most pore-forming immunotoxins, however, is their basal toxicity toward most cells, including red blood cells, which in turn prevents their pharmacologic use.

In nature, many toxins are synthesized as protoxin and activated by proteolytic removal of a polypeptide segment at either terminus. Cancer cells often overexpress specific tumor associated proteases, which are important for invasion and metastasis of cancer cells.[33,34] In one approach to reduce the toxicity toward healthy cells, immunotoxins have been prepared to specifically cleave the linker between the targeting moiety and the payload by intracellular cancer-associated proteases, hence activating the toxin *in situ*.[35,36] Pore-forming toxins have also be inactivated by genetic fusion with a polypeptide trigger and then proteolytically activated by cancer-associated proteases[37,38].

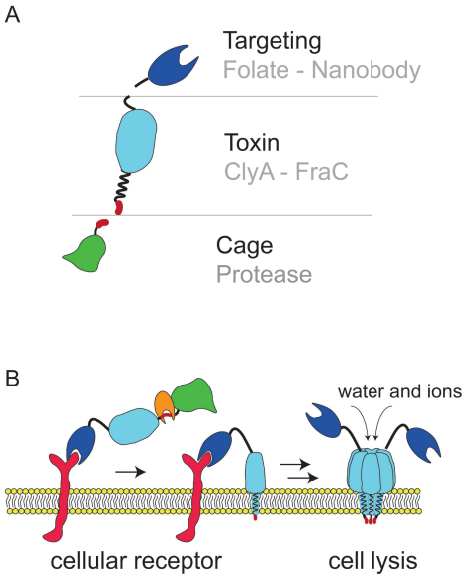

Figure 1. Modular nanopore immunotoxins. (**A**) Schematic representation of different modules used to build up a pore-forming immunotoxin with caged activity. The central point is the toxin. In this study we used the membrane-acting toxins ClyA and FraC. The C-terminus of the toxin was conjugated to different targeting molecules, including folate and an anti-EGFR nanobody, to direct the toxin to cancer cells. For site-specific activation of the toxin, DHFR was fused to the N-terminus of the toxin *via* a cancer protease sensitive linker. Activation of the toxin by proteolysis is necessary to enable pore-formation, and thus cell killing activity. (**B**) Schematic representation of the pore-formation of the designed protein drug. Soluble toxin is recruited to the host membrane by interactions of the targeting module and the corresponding receptor. Subsequent proteolytic cleavage at the specific protease site is necessary for activation of the toxin. Finally, the toxin can insert into the membrane. Pore-formation changes membrane permeability ultimately leading to cell death.

In this work, we describe the preparation of pore-forming immunotoxins consisting of a chemical or protein-based targeting element, a pore-forming toxin and a protease trigger (Figure 1). Crucially, each fusion step is optimized by directed evolution, which allowed tuning the toxicity toward the target cells, and efficient synthesis of the protein complexes in *E. coli* cells. We show a construct that recognizes a molecular target on cancer cells and is selectively activated by a cancer-associated protease, while displaying no off-target activity on other cells.

RESULTS AND DISCUSSION

Immunotoxin preparation by targeted chemical modification

Cytolysin A (ClyA) is a protein toxin synthesized as soluble 34 kDa monomeric protein, which assembles into a dodecameric pore causing the lysis of cell membranes rich in cholesterol [39]. In our first effort to prepare an immunotoxin, we conjugated folate to a cysteine residue introduced at position 272 in a previously engineered cysteine-less ClyA (ClyA-AS) from *Salmonella typhi*[40]. Folate was covalently attached to ClyA-AS-S272C monomers *via* a PEG-5K linker bearing a maleimide moiety (Figure 2A). SDS-PAGE revealed that about 50% of the ClyA-AS-S272C was conjugated (Figure 2B). The construct was purified by size exclusion chromatography and tested for cytotoxic activity on KB cells overexpressing folate receptors (FR). A MTT assay, which assesses the cell metabolism by measuring the mitochondrial potential, revealed that conjugation to folate increased toxicity toward FR^+ cells by about two-fold [IC_{50}(ClyA-folate) = 5.45 nM vs IC_{50}(ClyA) = 13.5 nM] (Figure 2C). In order to confirm that ClyA-folate induces preferential cell lysis, we added 10 nM of ClyA-folate to FR^+ and FR^- cells containing culture medium with a standard folate concentration (0.002 mM), and assessed the integrity of the cell membrane using a propidium iodide assay. Under these conditions we found that ClyA-folate causes increased cell death in FR^+ cells but not in FR^- cells (Figure 2D). This difference is abolished when folate concentration in the medium is increased 250-fold (Figure 2D). This suggests that cell death mediated by ClyA-folate is receptor mediated. Thus, conjugation of ClyA with folate increases its specificity to FR^+ cells, making this a possible candidate for a targeted therapy approach against FR-overexpressing tumors.

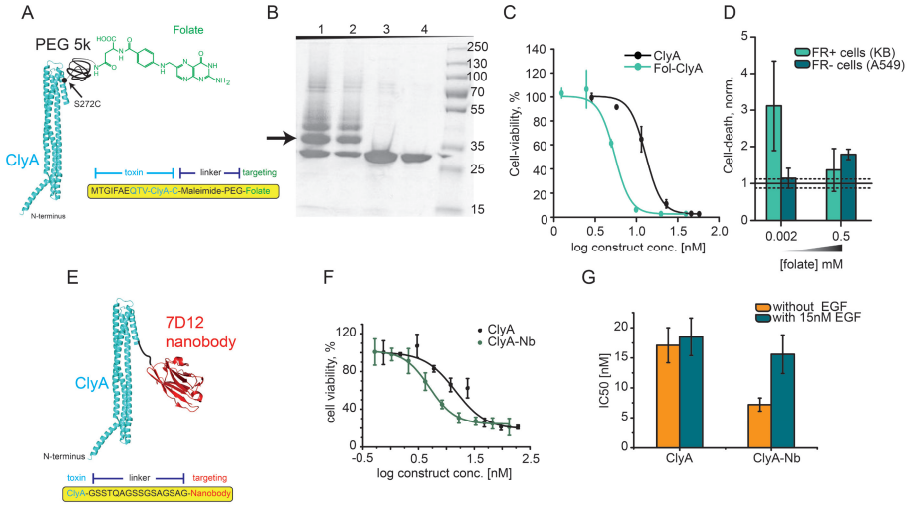

Figure 2. ClyA targeting cancer cells. (**A**) Schematic representation of ClyA (blue, PDB: 2WCD) conjugated to folate. Folate was covalently attached to ClyA-AS-S272C *via* a disulfide bond and a PEG linker. (**B**) ClyA folate conjugation examined by 12% SDS-PAGE electrophoresis. Lane 1 and 2: ClyA-AS-S272C modified with folate-5k PEG-maleimide showing about 50% modification. The arrow indicates modified ClyA-folate, the band below the arrow is un-modified ClyA, while additional bands above the arrow most likely represent additional incorporations of PEG-folate molecules reacting to lysine residues in ClyA-AS. Lane 3 and 4: ClyA-AS-S272C prior modification. (**C**) Comparison of IC_{50} of ClyA and ClyA-folate in FR-positive KB cells. (**D**) Comparison of cell death of FR-positive cells (KB) and FR-negative cells (A549) by 10 nM ClyA-folate, in standard medium (containing 0.002 mM of folate) and in medium supplemented with 250 fold higher folate concentration (0.5 mM). (**E**) Schematic representation of ClyA conjugated to nanobody at the C-terminus. ClyA is in blue the anti-EGFR nanobody 7D12 in red (PDB: 4KRL). (**F**) Representative dose-response curves of ClyA-AS and ClyA-Nb in the absence of EGF. Conjugation to the anti-EGFR nanobody increases toxicity toward EGFR overexpressing A431 cells. (**G**) Comparison of IC_{50} values of ClyA, and ClyA-Nb in the presence and absence of EGF.

A genetically encoded immunotoxin

In a second approach the anti-EGFR nanobody 7d12 [41,42] was genetically attached to the C-terminus of ClyA-AS *via* a 16 amino acid long linker (Figure 2E). EGFR-overexpression in cells is associated with different cancer types and is an indication of especially aggressive breast cancer[43,44]. The ClyA-AS-nanobody construct (ClyA-Nb) was overexpressed in *E. coli* cells and purified by Ni-NTA affinity chromatography. Conjugation to the nanobody preserved hemolytic activity of ClyA toward sheep red blood cells (Figure 3E, S2D). To test whether nanobody attachment improves toxicity toward EGFR-overexpressing cells, we measured the mitochondrial activity of A431 epidermoid carcinoma cells, overexpressing EGFR[45], at increasing concentration of immunotoxin. The cell viability experiments showed a two-fold reduced IC_{50} of ClyA-Nb [IC_{50} (ClyA-Nb) = 7.2 ± 1.1 nM] compared to ClyA-AS [IC_{50} (ClyA) = 17.1 ± 2.9 nM] (Figure 2F). Incubation with EGF abolished this difference (Figure 2G, S1A, S1B, S3A). Thus, as observed for ClyA-folate conjugation

the attachment of the targeting unit increased toxicity to the target cells by two-fold, making ClyA-Nb a possible candidate for a targeted therapy approach against EGFR-overexpressing tumors.

Protein engineering allows efficient synthesis in *E. coli* and improves targetability toward cancer cells

To increase specificity of ClyA toward the membranes of target cancer cells, we performed random-mutagenesis using degenerate primers targeting isoleucine 5 and phenylalanine 6 in ClyA-Nb (Figure 3A). The two residues are hydrophobic and are located just before the transmembrane region of ClyA. Thus, we hypothesized they are important for membrane binding. An initial negative screening on red blood cells was performed, where toxins which showed slower hemolysis rates than ClyA-Nb were selected. This step is intended to reduce the affinity of the toxin for non-target cell membrane. Moderate active variants were then purified by Ni-NTA affinity chromatography and tested for expression and purity by blue native polyacrylamide gel electrophoresis (BN-PAGE, Figure 3C, and S2A). Variants, which were highly expressed and showed no pre-oligomerization (*i.e.* they do not oligomerize in the absence of membranes or surfactants) were then selected and tested on A431 cells. Among the variants tested SE-ClyA-Nb could be purified with reasonably high yields (~ 1 mg from 300 mL culture), showed low tendency to pre-oligomerize, and showed a three-fold slower hemolytic activity compared to ClyA-AS and ClyA-Nb [t_{50} (ClyA-AS) = 12 min, t_{50} (ClyA-Nb) = 14 min, t_{50} (SE-ClyA-Nb) = 48 min for 1 μg toxin] (Figure S2D) . Crucially, the toxicity on A431 cells improved a further two-fold compared to ClyA-Nb [IC_{50} (SE-ClyA-Nb) = 4.1 ± 0.5 nM] (Figure 3F). In the presence of 15 nM, EGF the toxicity reduced four-fold [IC_{50} (SE-ClyA-Nb, EGF) = 16.0 ± 0.7 nM] (Figure 3G, S3B, S3C) to the level observed for ClyA [IC_{50} (ClyA, EGF) = 18.5 ± 3.1 nM] (Figure 3H), indicating that the additional toxicity of SE-ClyA-Nb is due to the specific interaction of the nanobody with the cancer cell receptors.

Toxins can be exchanged

The cytotoxic efficiency of ClyA toxins depends on the membrane composition of the targeted cell line. Thus, to refine and generalize our approach, we exchanged the ClyA nanopore toxin for the actinoporin Fragaceatoxin C (FraC). Similarly to ClyA, FraC is a pore-forming toxin that is expressed as water-soluble monomer and self-assembles into (octameric) transmembrane pores. However, the N-terminal membrane spanning region of FraC interact tightly with three sphingomyelin molecules per monomer (Figure S4A). Thus, FraC requires sphingomyelin to cause cell damage[46]. The anti-EGFR nanobody containing the 18-amino acid linker used to prepare ClyA-Nb was fused to the C-terminus of S-FraC to prepare S-FraC-Nb. S-FraC carries the

mutation W112S compared to wild type FraC that we found increased its expression in *E. coli* cells. S-FraC-Nb could be purified at high yield in *E. coli* cells and showed a similar hemolytic activity than S-FraC (Figure S4C), indicating that the protein fusion did not impair protein activity. As observed for ClyA, the fusion to the nanobody increases toxicity of S-FraC by two-folds toward EGFR-overexpressing cells [IC_{50} (S-FraC) 135.5 ± 22.7 nM, IC_{50} (S-FraC-Nb) = 63.9 ± 16.4 nM] (Figure S4D). Predictably, 15 nM of EGF reduced the toxicity of S-FraC-Nb [IC_{50} (S-FraC-Nb, EGF) = 197.9 ± 15.5 nM], but showed no effect on S-FraC [IC_{50} (S-FraC, EGF) = 138.5 ± 28.7 nM, (Figure S4E, S4F, S4G)].

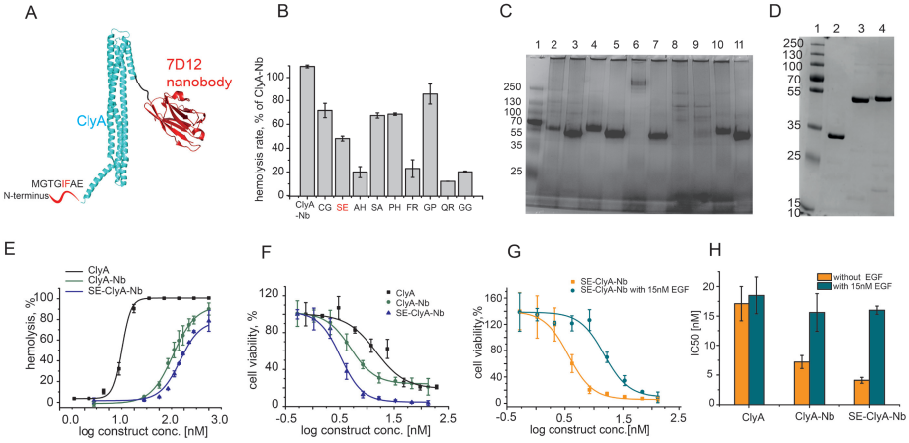

Figure 3. Directed evolution of ClyA-Nb. (**A**) Schematic representation of ClyA conjugated to nanobody. The amino acids at the N-terminus are not observed in the crystal structure of ClyA, suggesting they do not have a well-defined secondary structure. Amino acid 5 and 6, which were mutated to improve toxin properties, are shown in red. (**B**) Hemolytic activity of a part of the ClyA-Nb library. Hemolysis rates are presented as percentage of ClyA-Nb activity. (**C**) Part of the ClyA-Nb library analyzed by a 4-20% blue-native PAGE [40]. Lane 1: Protein ladder, lane 2: ClyA-Nb, lane 3: ClyA-Nb with 0.2% SDS, lane 4: SE-ClyA-Nb, lane 5: SE-ClyA-Nb with 0.2% SDS, lane 6: FR-ClyA-Nb, lane 7: FR-ClyA-Nb with 0.2% SDS, lane 8: QR-ClyA-Nb, lane 9: QR-ClyA-Nb with 0.2% SDS, lane 10: GG-ClyA-Nb, lane 11: GG-ClyA-Nb with 0.2% SDS. (**D**) ClyA-nanobody fusion purification examined by 12% SDS-PAGE. Lane 1: Protein ladder, Lane 2: ClyA, Lane 3: ClyA-Nb, Lane 4: SE-ClyA-Nb. (**E**) Comparison of the hemolysis percentage of ClyA and ClyA-Nb constructs. Fusion of ClyA to the Nb reduces hemolytic activity and the mutation I5S and F6E of ClyA reduces activity even further. (**F**) Toxicity of ClyA constructs toward EGFR overexpressing A431 cells, showing that both the nanobody and the additional mutation at the N-terminus improve toxicity toward the cells. (**G**) Toxicity of SE-ClyA-Nb in the presence and absence of 15 nM EGF, showing that the effect of the increased toxicity of SE-ClyA-Nb is due to the nanobody. (**H**) Comparison of IC_{50} values of ClyA, ClyA-Nb and SE-ClyA-Nb in the presence and absence of EGF, showing the high specificity of the SE-ClyA-Nb construct.

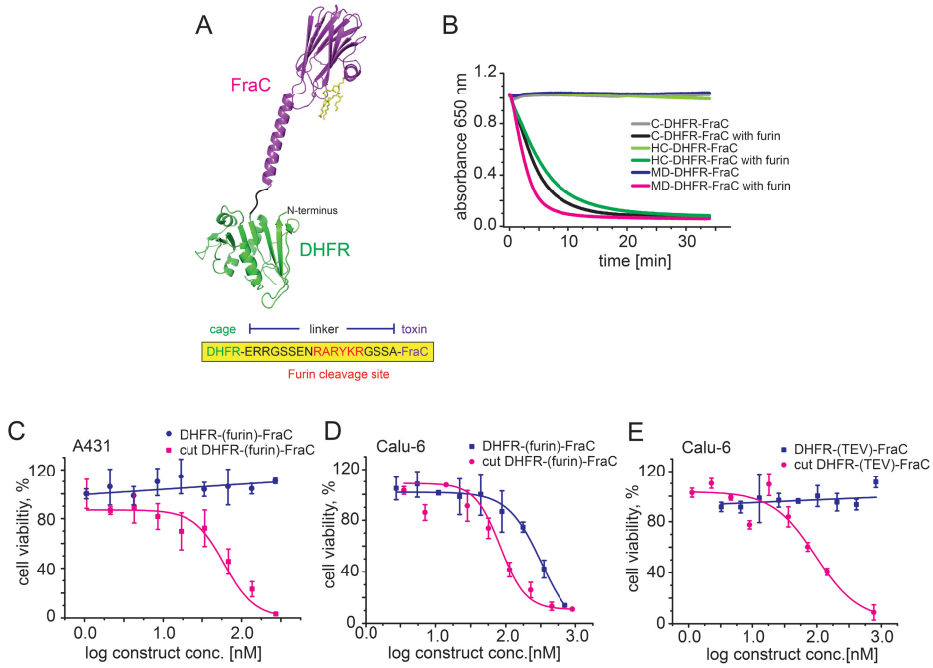

Figure 4. Caging FraC toxin. (**A**) Schematic representation of FraC conjugated to DHFR. FraC (purple, PDB: 4TSY) fused N-terminal to DHFR (green, PDB: 1RH3) by an 18 amino acid long linker including a protease cleavage site for furin. (**B**) Comparison of the hemolytic activity of different DHFR-FraC mutants resulted from directed evolution. Fusion of FraC to DHFR deactivates the toxin and therefore no hemolysis of red blood cells can be observed. Activation with the protease furin regains hemolytic activity of all mutants. (**C**) Representative dose-response curves of MD-DHFR-FraC and proteolysed MD-DHFR-FraC on A431 cells. Conjugation to DHFR deactivates the toxin, therefore no cell killing is observed for MD-DHFR-FraC. Proteolysis with furin triggers pore-formation of the toxin and recovers toxicity toward A431 cells. (**D**) Representative dose-response curves of MD-DHFR-FraC (DHFR-(furin)-FraC) and proteolysed MD-DHFR-FraC on Calu-6 cells. Calu-6 cells produce furin, which activates MD-DHFR-FraC resulting in cell killing (**E**) Representative dose-response curves of DHFR-(TEV)-FraC and proteolysed DHFR-(TEV)-FraC on Calu-6 cells. Conjugation to DHFR deactivates the toxin and Calu-6 cells do not express TEV proteases, therefore no cell killing is observed for DHFR-(TEV)-FraC. Proteolysis with TEV triggers pore-formation of the toxin and recovers toxicity toward Calu-6 cells.

A triggered toxin improved by directed evolution

Although directed evolution could increase the affinity of SE-ClyA-Nb for A431 cells while decreasing the toxicity toward red blood cells, the latter could not be completely abolished. Many tumor cells secrete proteases such as furin[34,47,48], urokinase plasminogen activator[49] or cathepsin B[50], which in turn activates other proteases, eventually promoting tumor metastasis by helping tumor cells digest the extracellular matrix and penetrate the basal lamina. Therefore, we planned to design an immunotoxin that is activated by furin. To silence the toxicity of ClyA we fused

dihydrofolate reductase (DHFR, 19 kDa) to the N-terminus of the ClyA-Nb and FraC-Nb toxins *via* a 18 amino acid long linker containing a furin cleavage site (Figure 4A, S5A). DHFR was selected because it is a relatively small protein that shows high water-solubility, express well in *E. coli* cells, and is non-toxic to human cells. The digestions of the constructs by furin will then remove DHFR thereby activating the toxin. Surprisingly, however, DHFR-SE-ClyA showed similar hemolytic activity as SE-ClyA-Nb, indicating that DHFR-SE-ClyA-Nb can oligomerize on membranes despite the large protein on the transmembrane helix (Figure S5C). By contrast, the DHFR-FraC construct was much less hemolytic active. However, the construct suffered from a small background activity on red blood cells, and could not be purified at high concentrations due to aggregation.

To improve the *E. coli* synthesis of the DHFR-FraC construct, we performed three rounds of random-mutagenesis on the entire construct. Libraries were generated by error-prone PCR and screened for hemolytic activity in the presence and absence of protease. Variants were selected which showed low or no background activity, but were hemolytic active after proteolytic cleavage. The best three variants from the third round were purified by Ni-NTA affinity chromatography and compared using hemolytic activity. MD-DHFR-FraC (displaying the T50M mutation on the DHFR sequence and the N325D mutation in the FraC sequence), C-DHFR-FraC (R312C at the interface of FraC protomers), and HC-DHFR-FraC (R102H in the active site of DHFR and R312C at the interface of FraC protomers) did not induce red blood cell lysis after addition of 10 μg of the purified proteins (Figure 4B, S6A). However, upon incubation with furin (three hours, 37 °C), all mutants lysed red blood cells within minutes [t_{50} (C-DHFR-FraC) = 4.8 min, t_{50} (HC-DHFR-FraC) = 5 min, t_{50} (MD-DHFR-FraC) = 2.8 min for 10 μg toxin] (Figure 4B). MD-DHFR-FraC was selected for further cytotoxic characterization on A431 cells. Addition of up to 600 nM DHFR-FraC caused no cell death, while equal concentration of proteolysed MD-DHFR-FraC showed cytotoxicity comparable to S-FraC [IC_{50} (cut FraC) = 98.9 ± 11.9 nM] (Figure 4C).

In order to test whether a DHFR-FraC construct can be activated by a cell-secreted protease, the MD-DHFR-FraC was tested on Calu-6 cells, a cell line expressing the protease furin,[51,52] a protease overexpressed by many cancer cells [34,51]. Rewardingly, MD-DHFR-FraC showed cytotoxicity on Calu-6 cells [IC_{50} 212.0 ± 35.4 nM] that was comparable to the pre-proteolysed MD-DHFR-FraC [IC_{50} 142.5 ± 30.5 nM] (Figure 4D). By contrast, when up to 820 nM of a caged immunotoxin containing a TEV (DHFR-(TEV)-FraC) rather than a furin cleavage site was used, no cytotoxic activity was observed (Figure 4E), indicating that the activation of FraC by Calu-6 cells was induced by furin and not by other nonspecific proteases.

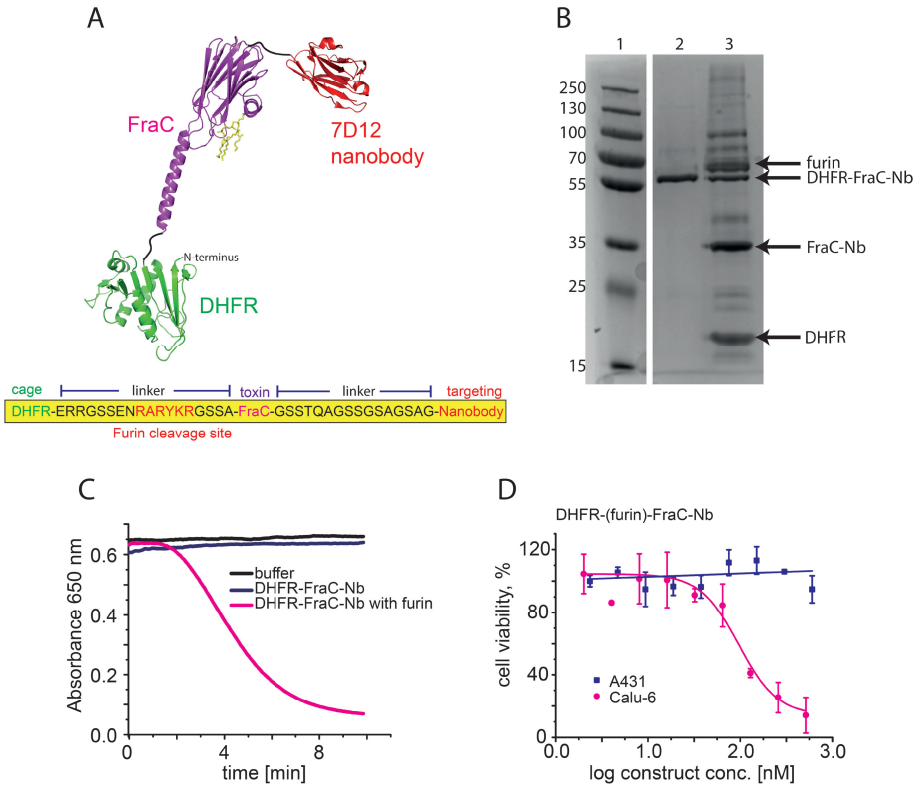

Figure 5. A caged pore-forming immunotoxin. (**A**) Schematic representation of FraC conjugated to DHFR and nanobody. FraC is in purple, DHFR in green and the C-terminal of anti-EGFR nanobody 7D12 in red. (**B**) 12% SDS-PAGE to examine DHFR-FraC-nanobody fusion and its proteolysis. Lane 1: Protein ladder, Lane 2: DHFR-FraC-Nb, Lane 3: DHFR-FraC-Nb proteolysed by furin (1:100 ratio). Only about 50% of DHFR-FraC-Nb was proteolytically activated. The arrows indicate the proteins of interest, while additional bands most likely correspond to partial proteolytic products or impurity in the commercial furin sample (**C**) Comparison of the hemolytic activity of DHFR-FraC-Nb and proteolysed DHFR-FraC-Nb. Only proteolysed DHFR-FraC-Nb is active. (**D**) Representative dose-response curves of DHFR-FraC-Nb toward A431 cells or Calu-6 cells, showing that DHFR-(furin)-FraC-Nb is only active on Calu-6 cells, which is the only cell line expressing furin necessary for activation.

A triggered immunotoxin

In the last step, the nanobody was genetically fused to the C-terminus of evolved MD-DHFR-FraC (Figure 5A). Although the size of the protein increased to 56 kDa, no additional directed evolution was required, as the construct successfully expressed well in *E. coli* cells (~ 1 mg from 300 mL culture) and could be efficiently purified in one-step by Ni-NTA affinity chromatography (Figure 5B). The full construct (DHFR-FraC-Nb) exhibited no hemolytic activity, while incubation with furin induced red blood cell lysis within a few minutes [t_{50} (DHFR-FraC-Nb) = 4.6 min for

10 µg toxin] (Figure 5C). As expected, DHFR-FraC-Nb was not cytotoxic toward A431 cells (24 h incubation) (Figure 5D), but caused cell death after incubation with furin [IC_{50} 146 ± 18.5 nM] (Figure S7B). Cytotoxicity was reduced when EGF was added to the growth medium [IC_{50} 283.9 ± 15.1 nM] (Figure SI 7C), confirming that the interaction with the cell membrane receptor increased the immunotoxin activity. *In situ* activation of DHFR-FraC-Nb was tested using the furin expressing cell line Calu-6 [51,52]. As expected, DHFR-FraC-Nb, which was not active on A431 cells, induced cell death toward Calu-6 cells [IC_{50} 95.2 ± 14.4 nM] (Figure 5D, S7B, and S7D). Addition of 15 nM EGF reduced the toxicity of DHFR-FraC-Nb by almost two-fold [IC_{50} 148.2 ± 3.6 nM] (Figure S7C, S7E). Most likely, the effect of the nanobody on Calu-6 cells is less pronounced because this cell line expresses less EGFR than A431 cells.[53]

DISCUSSION

Since the introduction of the first recombinant protein therapeutic, human insulin, 35 years ago, proteins have long remained a rarely used subset of medical treatments. In recent years protein therapeutics have increased dramatically in number and frequency of use, and have now a significant role in almost every field of medicine, despite this role is still only in its infancy. In this work, we describe a method that uses directed evolution to prepare protein-based therapeutic agents consisting of a membrane targeting element covalently linked to a caged toxin.

We tested ClyA from *Salmonella typhi* and FraC from *Actinia fragacea* pore-forming toxins as cytotoxic elements. Both toxins are expressed as soluble monomers that form oligomeric pores into lipid membranes. In order to direct protein toxicity toward selected cells we explored two approaches. A small molecule folate was chemically attached to ClyA via a 5 kDa PEG linker. The latter was used to mediate the interaction distance with the receptor and to facilitate the purification of the conjugate. This approach is fast and might allow screening hundreds of molecules. However, the bioorthogonal chemical linkages can be instable, and can produce low reaction yields that might result in heterogeneous samples. Thus, we tested a second approach where the variable antibody domains of single-domain camelid antibodies, called nanobodies (Nb), conjugated to the C-terminus of the toxin. Nanobodies are small and stable[54], penetrate tissues efficiently[55], show low immunogenicity [56] and can be easily produced in bacteria. For both approaches, we found that ClyA and FraC toxins conjugated to the targeting unit induced a two-fold increase of the IC_{50} toward cancer cell lines overexpressing the cognate receptor.

In order to improve the soluble expression of the immunotoxin, increase target affinity, and reduce the toxicity toward blood cells, we resorted to a directed evolution experiment in which

the hydrophobic residues at the N-terminus of the ClyA toxin were randomized. The rationale was that a reduced affinity of the immunotoxin for non-targeted membranes would be compensated by the nanobody-mediated binding to a specific membrane target, leading to a greater difference in toxicity between cell types. Using this approach, we identified pore-forming immunotoxins with an additional two-fold increased IC_{50} toward cells expressing EGFR and a three-fold reduced off-target hemolytic activity. Simultaneously, the production yield in *E. coli* cells was more efficient.

In the final step, we sought to completely suppress off-target activity. In nature, many toxins are synthesized as protoxins that are proteolytically activated extracellularly. Borrowing from nature, we introduced a polypeptidic segment at the transmembrane N-terminus of FraC and ClyA to cap the activity of the nanopore toxins. The conjugate was preceded by a cleaving sequence for furin, which is a cancer-associated protease involved in degrading the extracellular matrix in tumor formation and metastasis [57]. We found that ClyA was fully active on red blood cells [58], while the toxicity of FraC was reduced but not completely abolished. Gladly, the toxicity of the caged FraC-Nb toxin could be suppressed by three rounds of directed evolution, allowing identifying a construct that was completely inactive toward cellular membranes but fully active upon *in situ* protease activation by a cancer cell line over-expressing furin.

This work describes a method that uses a directed evolution approach to prepare pore-forming immunotoxins with caged activity. Our design contains three separate elements that can be easily exchanged: a water-soluble pore-forming toxin that oligomerizes on lipid membranes, a membrane targeting unit, and protein trigger for *in situ* activation. The targeting element and the protein trigger allows a two-degree control of the toxin activity. The pore-forming ability of the immunotoxin may offers advantages compared to conventional toxins. The activity can be easily assayed on red blood cells, which in turns allows using random mutagenesis approaches to improve the synthesis of the proteins in *E. coli* cells and to fine-tune the properties of the protein conjugate. In addition, the oligomeric nature of the assembled cytotoxic pores will allow conjugating the protein drug with multiple membrane targeting motives, which will allow further fine-tuning of the cytotoxicity toward targeted cells.

MATERIALS AND METHODS

Unless otherwise specified, all chemicals were bought from Sigma-Aldrich. DNA was purchased from Integrated DNA Technologies (IDT). Enzymes were acquired from Fermentas. All errors are given as standard deviations.

Cloning

ClyA-nanobody cloning

A Xho I restriction site (CTCGAG) was introduced at the 3' end of ClyA-AS gene [40] inserted into a T7 expression plasmid (pT7-SC1) [59] by PCR using ClyAXr and ClyAXf primers (Table S1, PCR conditions 1, Table S2). Separately, the synthetic gene encoding for the a EGFR recognizing nanobody 7d12 [41], which included a His_6- at the 3' end and a 16 amino acid glycine, alanine and serine linker (underlined in the sequence) at the 5' end, was amplified by PCR using Nbr and Nbf as primer (Table S1, PCR condition 1, Table S2). Then the newly constructed DNA plasmid containing ClyA-AS and the DNA construct containing the nanobody were purified with QIAquick PCR Purification Kit (Qiagen), digested with Xho I and Hind III, and ligated together using T4 ligase (Fermentas). 0.5 µL of the ligation mixture was transformed into 50 µL of *E. cloni*® 10G cells (Lucigen) by electroporation. The transformed bacteria were grown overnight at 37 °C on ampicillin (100 µg mL^{-1}) LB agar plates. The identity of the clones was confirmed by sequencing.

Construction of saturation mutagenesis library of ClyA-nanobody

The library was constructed by saturation mutagenesis of position 5 and 6 of ClyA-nanobody. For mutagenesis we used the plasmid encoding for ClyA-nanobody as a template. DNA amplification was performed using PCR condition 2 (Table S2), the T7 terminator primer (Table S1), and a primer containing a degenerated codon at position 5 and 6 encoding for the complete set of amino acids (Table S1). The PCR products were pooled together, gel purified (QIAquick Gel Extraction Kit, Qiagen) and cloned into pT7-SC1 by the MEGAWHOP procedure [60]: ~500 ng of the purified PCR product was mixed with ~300 ng of pT7-SC1 plasmid containing ClyA-nanobody gene and the amplification was carried out with Phire Hot Start II DNA polymerase (Finnzymes) using PCR condition 3 (Table S2). The circular template was eliminated by incubation with Dpn I (1 FDU) for 2 hours at 37 °C. 0.6 µL of the resulting mixture was transformed into 50 µL of *E. cloni*® 10G cells (Lucigen) by electroporation. The transformed bacteria were grown overnight at 37 °C on ampicillin (100 µg mL^{-1}) LB agar plates typically resulting in $>10^5$ colonies which were harvested for plasmid DNA library preparation.

Construction of ClyA S272C

ClyA S272C was obtained from a pT7-SC1 plasmids containing the ClyA-AS gene which served as templates for Quick-Change PCR (PCR condition 1, Table S2) using the primers S272Cf and S272Cr (Table S1). The PCR product was purified using QIAquick PCR purification kit (Qiagen) and the circular template was eliminated by incubation with Dpn I (1FDU) for 1 hour at 37 °C. The mixture (0.5 µL) was transformed into 50 µL of *E. cloni*® 10G cells (Lucigen) by electroporation.

The transformed bacteria were grown overnight at 37 °C on ampicillin (100 μg mL^{-1}) LB agar plates. The identity of the clones was confirmed by sequencing.

Construction of S-FraC

S-FraC was prepared by using pT7-SC1 plasmid containing WtFraC gene [61] as template for a PCR reaction using W112SFf and T7 terminator primers (Table S1), and PCR condition 2 (Table S2). The PCR product was purified using QIAquick PCR purification kit (Qiagen) and cloned into pT7-SC1 by the MEGAWHOP procedure using pT7-SC1 plasmid containing WtFraC gene as template and the purified PCR product as primers.

Construction of S-FraC-nanobody

Part of the 16 amino acid glycine, alanine and serine linker (underlined in the sequence) was introduced at the 3' end of S-FraC by PCR using the T7 promoter and primer FNlinkr (Table S1, PCR condition 2, Table S2). The DNA construct was then gel purified (QIAquick Gel Extraction Kit, Qiagen). ~500 ng then served as primers for a second PCR reaction that used the pT7-SC1 plasmid containing the His_6-tagged ClyA-nanobody gene as template for cloning by the MEGAWHOP procedure.

DHFR-FraC cloning

A synthetic gene encoding for DHFR[62] from *E. coli* (N-terminal end) and FraC containing the additional mutations D10G and K159E spaced by a 18 amino acid long linker (underlined in the DNA sequence at the end of the method section) and a His_6-tag at the C-terminus was bought from IDT. The synthetic gene was amplified by PCR using primers DFf and DFr (Table S1) and PCR condition 1 (Table S2). The PCR product was purified by QIAquick PCR purification kit (Qiagen), digested with Nco I and Hind III (FastDigest, Fermentas), ligated into a pT7-SC1 expression plasmid using T4 ligase (Fermentas) transformed into 50 μL of *E. cloni*® 10G cells (Lucigen) by electroporation.

Construction of DHFR-FraC-nanobody

The gene of MD-DHFR-FraC was amplified using T7 promotor, primer DFnHr (Table S1), and PCR condition 2 (Table S2). In a second PCR reaction FraC-nanobody gene was amplified using T7 terminator, primer DFnHr (Table S1) and PCR condition 2 (Table S2). Both PCR products were purified with QIAquick PCR purification kit (Qiagen). 50 ng of both purified PCR products, which contain an overlapping sequence, were used as template for a third PCR reaction using T7 promotor, T terminator (Table S1) and PCR condition 2 (Table S2). The resulting PCR product

encoding His_6-tagged DHFR-FraC-nanobody gene was digested, ligated and transformed as described in section: "construction of DHFR-FraC".

Construction of DHFR-ClyA

The gene of DHFR-FraC was amplified by PCR using the T7 promoter, primer DHFRlinkr (Table S1), and PCR condition 2 (Table S2). In a second PCR reaction the gene of ClyA was amplified using LinkClyA and ClyAr as primers (Table S1), and PCR condition 2 (Table S2). 50 ng of both constructs, which contain an overlapping sequence, are then the template for a third PCR reaction (PCR condition 2, Table S2) using T7 promotor and ClyAr (Table S1) as primers. The final construct was digested with Nco I and Hind III (FastDigest, Fermentas) and cloned into pT7-SC1 expression plasmid.

Construction of DHFR-FraC library by error-prone PCR

Libraries were constructed by amplifying the DHFR-FraC gene from plasmid DNA using T7 promoter and T7 terminator (Table S1). In the first round of mutagenesis we used a plasmid encoding for DHFR-FraC as template. DNA amplification was performed by error-prone PCR with 0-0.2 mM $MnCl_2$ using T7 promoter and T7 terminator (Table S1) primers and PCR condition 2 (Table S2). The PCR products were pooled together, gel purified (QIAquick Gel Extraction Kit, Qiagen) and cloned into a pT7 expression plasmid (pT7-SC1) by the MEGAWHOP procedure using the purified PCR product and pT7-SC1 plasmid containing DHFR-FraC gene for amplification as described above in section: "construction of ClyA-nanobody library". Typically, $>10^5$ colonies were obtained, which were harvested for plasmid DNA library preparation. For the second round of mutagenesis we used the DNA plasmids that were derived from the previous round of selection (section: "Hemolytic screening DHFR-FraC libraries"), and used the conditions for DNA amplification by error-prone PCR using template concentrations of 0.1–400 ng [63], and PCR condition 2 (Table S2) using T7 promoter and T7 terminator (Table S1) as primers. These conditions typically yielded in 1 – 4 mutations per gene in the final library. The PCR products were pooled together and handled as described in the previous paragraph. For the third round of mutagenesis we used the DNA plasmids that were derived from the previous round of selection and we changed the protease cleavage site from TEV to furin. In contrast to TEV, furin is cancer associated protease. DNA amplification was performed by PCR condition 2 (Table S2) using primer Furf and T7 terminator (Table S1). These conditions typically yielded in 0 – 2 mutations per gene in the final library. The PCR products were pooled together, gel purified (QIAquick Gel Extraction Kit, Qiagen) and cloned into a pT7 expression plasmid (pT7-SC1) by the MEGAWHOP procedure using the purified PCR product and pT7-SC1 plasmid containing pT7-SC1 plasmid containing DHFR-FraC gene for amplification.

Protein expression

E. cloni® EXPRESS BL21 (DE3) cells were transformed with the pT7-SC1 plasmid containing the appropriate gene. Transformants were selected after overnight growth at 37 °C on LB agar plates supplemented with 100 mg L^{-1} ampicillin. The resulting colonies were inoculated in 10 mL 2xYT medium containing 100 mg L^{-1} of ampicillin. The culture was grown at 37 °C, with shaking at 200 rpm, until it reached an OD_{600} of ~0.6. The expression of protein was induced by the addition of 0.5 mM IPTG and the growth was continued at 21 °C. The next day the bacteria were harvested by centrifugation at 6000*xg* for 30 minutes and pellets were stored at -80 °C.

Protein purification

Periplasmic purification of ClyA and ClyA-nanobody

The pellets containing ClyA-AS or ClyA-nanobody were resuspended in 25 mL of 15 mM Tris. HCl pH 7.5, 1 mM Ethylenediaminetetraacetic acid (EDTA) and 20 % sucrose. Then the bacteria suspension was subjected to vigorous shaking at ambient temperature for 30 minutes. The bacterial cells were harvested by centrifugation at 6000*xg* for 15 minutes. The supernatant was discarded and the pellet resuspended in 10 mL 5 mM $MgCl_2$ supplemented with 0.05 units mL^{-1} of DNase I (Fermentas) and shacked for 1 hour. The cell suspension was centrifuged at 6000*xg* for 20 minutes. The supernatant was supplemented with 10 mM imidazole and mixed with 200 µL (bead volume) of Ni-NTA resin (Qiagen) that was pre-equilibrated with wash buffer (10 mM imidazole 150 mM NaCl, 15 mM Tris.HCl pH 7.5). After 45 minutes the resin was loaded into a column (Micro Bio Spin, Bio-Rad) and washed with ~10 mL of wash buffer. ClyA- AS or ClyA-nanobody was eluted with approximately 300 µL of wash buffer containing 300 mM imidazole. Protein concentration was determined by Bradford assay and toxin monomers were stored at 4 °C until further use.

Cytosolic purification of proteins (ClyA-S272C, S-FraC, S-FraC-nanobody, DHFR-(TEV)-FraC, MD-DHFR-FraC, DHFR-ClyA and DHFR-FraC-nanobody)

The pellets containing overexpressed proteins were thawed and resuspended in 20 mL of 15 mM Tris.HCl pH 7.5, 150 mM NaCl, 10 mM imidazole, 1 mM $MgCl_2$ and 0.05 units mL^{-1} of DNase I (Fermentas). Then, to initiate cell disruption, the bacteria suspension was supplemented with 0.2 mg mL^{-1} lysozyme and a cOmplete™, Mini, EDTA-free Protease Inhibitor Cocktail tablet (Roche) and was subjected to vigorous shaking at ambient temperature for 1 hour. The remaining bacteria were disrupted by probe sonication. The crude lysates were clarified by centrifugation at 6000*xg* for 30 minutes and supernatant mixed with 200 µL (bead volume) of Ni-NTA resin (Qiagen) that was pre-equilibrated with wash buffer (10 mM imidazole 150 mM NaCl, 15 mM Tris.HCl pH 7.5). After 45 minutes of gentle mixing at ambient temperature, the resin was loaded onto a column (Micro Bio Spin, Bio-Rad) and washed with ~10 mL of wash buffer. S-FraC or S-FraC-nanobody was eluted

with approximately 300 µl of wash buffer containing 300 mM imidazole. Protein concentration was determined by Bradford assay. All monomers were stored at 4 °C until further use.

Purification of ClyA-AS-S272C was performed as described in the section above, however, to avoid oxidation of the cysteine 5 mM Tris(2-carboxyethyl)phosphine (TCEP) was added until the final step, which included the washing of the Ni-NTA resin with 10 mL wash buffer supplemented with 5 mM TCEP. One additional step was then performed, in which the resin was washed with the same buffer (~10 mL) but without the reducing agent. ClyA-AS-S272C was eluted with approximately 150 µL of wash buffer containing 300 mM imidazole. Immediately after elution from the Ni-NTA resin, the ClyA-AS-S272C monomer was mixed with 20-fold molar excess of Folate-5k PEG-maleimide (Nanocs), dissolved in 15 mM Tris.HCl pH 7.5, 150 mM NaCl and the reaction was allowed to proceed for 2 hours at room temperature or at 4 °C overnight. According to SDS-PAGE analysis, ~50 % of the ClyA monomers were modified. ClyA-monomers conjugated to folate were separated from unmodified monomers and unreacted Folate-5k PEG-maleimide by gel filtration using 15 mM Tris.HCl pH 8.0, 150 mM NaCl buffer.

Purification of DHFR-ClyA was performed as described for S-FraC above, however, an additional purification step was necessary, because DHFR-ClyA forms inclusion bodies. Therefore, after clarifying the crude lysate by centrifugation, the resulting pellet was resuspended in ~20 mL wash buffer supplemented with 8 M urea. The cell suspension was centrifuged at 6000*xg* for 20 minutes and the supernatant His-Tag purified as described above, while washing the urea concentration was decreased gradually from 8M to 0M.

DHFR-(TEV)-FraC and MD-DHFR-FraC was expressed and lysed as described for S-FraC above. Instead of His-Tag purification using gravity-flow chromatography, the clarified lysate was applied to a HisTrap HP column (GE Healthcare Life Science) connected to Äkta pure chromatography system (GE Healthcare Life Science) which was equilibrated before with wash buffer (30 mM imidazole, 15 mM Tris.HCl and 500 mM NaCl). DHFR-(TEV)-FraC and MD-DHFR-FraC was eluted with wash buffer containing 500 mM imidazole. DHFR-(TEV)-FraC and MD-DHFR-FraC was eluted with wash buffer supplemented with 500 mM imidazole. FraC was then obtained from either DHFR-(TEV)-FraC or MD-DHFR-FraC by injecting 0.5 mL trypsin (1 mg mL^{-1}) from bovine pancreas, which cleaves off DHFR and then the column was washed to elute free DHFR and trypsin. Cut FraC was eluted with wash buffer supplemented with 500 mM imidazole.

Purification of DHFR-ClyA and DHFR-FraC-nanobody was performed as described for S-FraC above. FraC-nanobody could also be obtained by proteolysis from DHFR-FraC-nanobody, in

which case 1 unit furin was added per 25 µg DHFR-FraC-nanobody and incubated overnight at ambient temperature.

Hemolytic activity assay

Defibrinated sheep blood (ThermoFisher Scientific) was washed with 150 mM NaCl, 15 mM Tris.HCl pH 7.5 until the supernatant was clear. The erythrocytes were then resuspended with the same buffer to ~1 % concentration (OD_{650} 0.6 – 0.8). The suspension (120 µL) was then mixed with the solutions containing toxin. Hemolytic activity was measured by monitoring the decrease in OD_{650} using the Multiskan™ GO Microplate spectrophotometer (ThermoFisher Scientific). Hemolytic activity of 1 µg ClyA-AS, 1 µg ClyA-nanobody, 1 µg S-FraC and 1 µg S-FraC-nanobody was measured as described above. Hemolysis rate was calculated as inverse of the time elapsed till 50% decrease in turbidity.

To determine hemolytic activity of DHFR-ClyA or DHFR-FraC, 10 µg of toxin was mixed with 0.1 µg trypsin in 100 µL buffer (150 mM NaCl, 15 mM Tris.HCl pH 7.5, 1 mM $CaCl_2$) and incubated 5 minutes before applying to the erythrocyte solutions. As control the same experiment was performed using the same buffer without trypsin. Similarly, solutions containing DHFR-FraC-nanobody were activated using 0.1 µg of furin (PeproTech) instead of trypsin.

The concentration dependency of hemolytic activity, measured for ClyA and ClyA-nanobody, was tested by preparing different toxins concentrations in a final volume of 100 µL buffer (150 mM NaCl, 15 mM Tris.HCl pH 7.5). Then the addition of 120 µL washed 1 % erythrocyte solution was added. After 60 minutes incubation at room temperature hemolysis was recorded by measuring absorbance at 650 nm.

Hemolytic screening of ClyA-nanobody libraries

For screening, plasmid DNA of the library was transformed into *E. cloni*® EXPRESS BL21 (DE3) (Lucigen). 384 clones were randomly picked and individually grown in 96-deep-wells plates overnight by shaking at 37 °C (0.5 mL 2xYT medium containing 100 µg mL^{-1} ampicillin). The obtained cultures were used as starters for protein overexpression. 50 µL of the overnight starter cultures were inoculated into 500 µL of fresh medium in new 96-deep-well plates and cultures were grown at 37 °C until an optical density of 600 nm (OD_{600}) of about 0.6. Then, Isopropyl-β-D-thiogalactopyranoside (IPTG, 0.5 mM) was added to induce overexpression and the temperature was reduced to 25 °C for an overnight incubation. Bacteria were harvested the following day by centrifugation at 3000*xg* for 15 minutes at 4 °C. The supernatant was discarded and pellets were frozen at -80 °C for two hours to facilitate cell disruption. Cell pellets were then resuspended in

500 µL of lysis buffer (15 mM Tris.HCl pH 7.5, 1 mM $MgCl_2$, 10 µg mL^{-1} lysozyme, 0.2 units mL^{-1} DNase I) and lysed by shaking at 1300 rpm for 1 hour. The cell suspension was centrifuged at 3000*xg* for 20 minutes. Hemolytic activity using 10 µL of the crude lysate was determined as above described in section: "hemolytic activity assay". Active variants that showed slower hemolysis rates than ClyA-Nb were selected and the corresponding starter culture was used to obtain the plasmid DNA. The identity of the clones was confirmed by sequencing. Sequence changes that occurred in the corresponding genes are summarized in Table S3.

Hemolytic screening DHFR-FraC libraries

Libraries of DHFR-FraC were created and transformed into *E. coli* BL21 (DE3) and grown in 96 microwell plates as described above in the section: "screening of ClyA-nanobody libraries". In each round of selection, 768 individual clones were tested for hemolytic activity. In the first two selection rounds, two aliquots of 10 µL of crude lysate were tested for hemolytic activity. One aliquot was pre-incubated with trypsin (10 µL, 0.5 mg mL^{-1}, 5 min incubation time), the other was tested directly on red blood cells as described in "screening of ClyA-nanobody libraries". Clones with no or low background activity (t_{50} > than ~60 minutes) and high hemolytic activity after proteolysis (t_{50} < 10 min) were selected and the corresponding starter culture was used to obtain the plasmid DNA. In the third round of screening furin, (3 hours pre-incubation time at 37 °C, 0.01 mg mL^{-1} final furin concentration) was used instead of trypsin. The identities of the clones were confirmed by sequencing. Sequence changes that occurred in the corresponding genes are summarized in Table S4.

Cell viability assay

The cell viability assays were performed with the Human squamous carcinoma cell line A431 (Sigma-Aldrich). Detached cell number was determined by cell counting using an improved Neubauer chamber. The viability of cells was measured using (2-2-methoxy-4-nitrophenyl)-5-(2,4-disulfophenyl)-2H-tetrazolium, monosodium salt (WST-8) based cell viability assay included in the Cell Counting Kit-8 (CCK-8, Sigma-Aldrich) according to the manufacture's instructions.

The human squamous carcinoma cell line A431 (Sigma-Aldrich) and the human lung adenocarcinoma cell line Calu-6 (Cell Lines Service) were routinely maintained at 37 °C, in a humidified incubator under 5 % CO_2. A431 cells and Calu-6 cells were grown in Dulbecco's Modified Eagle Medium (DMEM) supplemented with 10 % Fetal Bovine Serum (FBS), 2 mM glutamine, and 100 µg mL^{-1} gentamycin.

A431 cells were first detached with 5 mL of 0.25 % Trypsin/EDTA solution, centrifuged at 400*xg* for 5 minutes, and suspended in 10 mL growth medium, counted as described above and seeded

20.000 cells per well in 96-well tissue culture plates in 200 µL growth medium and incubated overnight at 37 °C in 5 % CO_2 atmosphere. Either 2 µL epidermal growth factor (EGF, final concentration 15 nM) or PBS was added to each well. In various concentrations 10 µL toxin was distributed to the cells and incubated 24 hours at 37 °C in 5 % CO_2 atmosphere. Cells with only medium were included as control. Next, 5 µL CCK-8 solution was added to each well and the plates were incubated 2 hours before measuring absorbance at 450 nm using the Multiskan™ GO Microplate spectrophotometer (ThermoFisher Scientific).

Calu-6 were first detached with 5 mL of 0.25 % Trypsin/EDTA solution, centrifuged at 300*xg* for 5 minutes, and suspended in 10 mL growth medium, counted as described above and seeded 20.000 cells per well in 96-well tissue culture plates in 200 µL growth medium and incubated overnight at 37 °C in 5 % CO_2 atmosphere. In various concentrations 10 µL toxin was distributed to the cells and incubated 48 hours at 37 °C in 5 % CO_2 atmosphere. Cells with only medium were included as control. Next, 5 µL CCK-8 solution was added to each well and the plates were incubated 2 hours before measuring absorbance at 450 nm using the Multiskan™ GO Microplate spectrophotometer (ThermoFisher Scientific).Results are shown as percentage of control cells and represented as average ± standard deviation of 3 independent experiments with triplicates.

For the kinetic experiments A431 cells were seeded in 96-well tissue culture plates as described above. Either 2 µL epidermal growth factor (EGF, final concentration 15 nM) or PBS was added to each well. Each hour one column of the plate was treated with 16 nM SE-ClyA-nanobody toxin. The viability of the cells was measured one hour after the last toxin addition.

Cell viability assay ClyA-folate

KB (folate receptor positive, FR+) cells (kindly supplied by Andreia Gomes, Universidade do Minho, Portugal) and A549 (FR-) cells (kindly supplied by Dr Maria João Amorim, Instituto Gulbenkian de Ciência, Portugal) were routinely maintained at 37 ºC, in a humidified incubator under 5 % CO_2. Both cell lines were grown in RPMI 1640 supplemented with 10 % FBS, 1 % GlutaMAX, 1 % NEAA, 1 % HEPES, 1 % Pen-Strep (all reagents from Gibco, Life Technologies, USA), a medium further referred to as "complete RPMI".

KB cells or A549 cells were seeded in a 96 well plate, at a density of 10 000 cells/well and incubated for 24 hours to allow for cell attachment. Cells were treated with either ClyA-AS (stock solution in 25% glycerol, 7.5 Tris.HCl pH 8.0 75 mM NaCl and 150 mM imidazole) or ClyA-AS-S272C (stock solution in 25% glycerol, 7.5 Tris.HCl pH 8.0 75 mM NaCl) for 24 hours. Upon end of the incubation period, 50 µg/well of 3-(4,5-dimethylthiazol-2-yl)-2,5-diphenyl tetrazolium bromide

(MTT) was added to all wells (except for 3 wells, which contained only medium and were used as blank controls), and the cells were returned to the incubator for another 4 hours. After this time, the medium was removed by inverting the plate and 200 µL of dimethyl sulfoxide (DMSO) to solubilize the resulted formazan was added per well. Absorbance at 540 nm was measured (and 690 nm was used as reference wavelength) using a Tecan Infinite M200 plate-reader. Results are shown as percentages of controls (i.e. vehicles) and represent, unless otherwise stated, average ± SEM (of 2 or 3 independent experiments with technical triplicates).

For the Folate Competition Assays, cells were seeded as described above, in "complete RPMI" medium without folate. After 24 hours of incubation, cells were incubated in medium supplemented with 0.002 (i.e. [folate] commonly found in RPMI 1640) or 0.5 mM of folic acid and treated with 11.5 nM ClyA-AS-S272C. After 24 hours of treatment, either a MTT assay or a propidium assay was performed (see below).

Propidium iodide assay

Cells were seeded in 24 well-plates at 30,000 cells/well in RPMI 1640 without folate, supplemented as described above, and incubated for 24 hours to allow for attachment. After this time, the medium was switched according to the above description of the Folate Competition Assays. After 24 hours of treatment, cells were harvested after trypsinization (TrypLE Express, Life Technologies, USA) into FACs tubes and washed twice with 1x Phosphate Buffered Saline (PBS). Cells were then resuspended in 5 µg mL^{-1} of propidium iodide solution (in 10 % FBS in 1x PBS) and after 15 minutes fluorescence was measured using a LSR Fortessa cytometer equipped with a 488 nm laser and a 575/26BP + 550LP combination of filters. Results are shown as percentages of controls (i.e. "vehicles") and represent, unless otherwise stated, average ± SEM (of 2 or 3 independent experiments with technical triplicates).

>ClyA-nanobody (protein sequence)

MGTGIFAEQTVEVVKSAIETADGALDLYNKYLDQVIPWKTFDETIKELSRFKQEYSQEASV
LVGDIKVLLMDSQDKYFEATQTVYEWAGVVTQLLSAYIQLFDGYNEKKASAQKDILIRILD
DGVKKLNEAQKSLLTSSQSFNNASGKLLALDSQLTNDFSEKSSYYQSQVDRIRKEAYAGAAA
GIVAGPFGLIISYSIAAGVIEGKLIPELNNRLKTVQNFFTSLSATVKQANKDIDAAKLKLATEI
AAIGEIKTETETTRFYVDYDDLMLSLLKGAAKKMINTSNEYRQRHGRKTLFEVPDVGSSTQ
AGSSGSAGSAGQVKLEESGGGSVQTGGSLRLTCAASGRTSRSYGMGWFRQAPGKEREFVSG
ISWRGDSTGYADSVKGRFTISRDNAKNTVDLQMNSLKPEDTAIYYCAAAAGSAWYGTLYE
YDYWGQGTQVTVSSGSAGSSHHHHHH*

>ClyA-nanobody (DNA sequence)

CCATGGGTACGGGTATCTTTGCGGAACAGACGGTGGAAGTTGTGAAAAGTGCGATT
GAAACGGCTGACGGTGCGCTGGACCTGTATAATAAATATCTGGATCAGGTCATCCCG
TGGAAAACCTTTGACGAAACGATTAAAGAACTGAGCCGTTTCAAACAGGAATACAG
TCAAGAAGCGTCCGTCCTAGTGGGCGATATCAAAGTGCTGCTGATGGATTCTCAGGA
CAAATATTTTGAAGCTACCCAAACGGTTTACGAATGGGCGGGTGTGGTTACCCAGCT
GCTGTCCGCATATATTCAGCTGTTCGATGGATACAATGAGAAAAAAGCGAGCGCGCA
GAAAGACATTCTGATCCGCATTCTGGATGACGGCGTGAAAAAACTGAATGAAGCCC
AGAAATCGCTGCTGACCAGCTCTCAATCATTTAACAATGCCTCGGGTAAACTGCTGG
CACTGGATAGCCAGCTGACGAACGACTTTTCTGAAAAAAGTTCCTATTACCAGAGCC
AAGTCGATCGTATTCGTAAAGAAGCCTACGCAGGTGCCGCAGCAGGTATTGTGGCCG
GTCCGTTCGGTCTGATTATCTCATATTCAATTGCTGCGGGCGTTATCGAAGGTAAAC
TGATTCCGGAACTGAACAATCGTCTGAAAACCGTTCAGAACTTTTTCACCAGTCTGT
CTGCTACGGTCAAACAAGCGAATAAAGATATCGACGCCGCAAAACTGAAACTGGCC
ACGGAAATCGCTGCGATTGGCGAAATCAAAACCGAAACGGAAACCACGCGCTTTTA
TGTTGATTACGATGACCTGATGCTGAGCCTGCTGAAAGGTGCCGCGAAGAAAATGA
TTAATACCTCTAATGAATATCGGCAGCGTCACGGTAGAAAAACCCTGTTTGAAGTCC
CGGATGTGGGCAGCAGCACTCGAGCGGGCTCCTCGGGTTCGGCGGGTTCGGCGGGT
CAAGTCAAACTGGAAGAATCAGGTGGTGGCTCGGTTCAAACGGGCGGCAGCCTGCG
CCTGACCTGTGCCGCATCTGGTCGTACGAGCCGCTCTTACGGCATGGGTTGGTTTCG
TCAGGCGCCGGGTAAAGAACGCGAATTCGTCAGTGGTATTTCCTGGCGCGGCGATT
CAACCGGTTATGCGGACTCGGTGAAAGGTCGTTTTACCATCTCCCGCGATAACGCCA
AAAATACGGTTGACCTGCAGATGAACAGCCTGAAACCGGAAGATACGGCAATTTATT
ACTGTGCAGCTGCGGCCGGCAGTGCTTGGTACGGTACCCTGTATGAATACGACTATT
GGGGCCAAGGTACGCAAGTCACGGTCTCTTCAGGTTCAGCGGGCTCGTCGCACCAT
CACCATCACCACTGATAAAAGCTTGGATCCGGC

>DHFR-ClyA (protein sequence)

MAHHHHHGSAMISLIAALAVDRVIGMENAMPWNLPADLAWFKRNTLDKPVIMGRHMW
ESIGRPLPGRKNIILSSQPGTDDRVTWVKSVDEAIAAAGDVPEIMVIGGGRVYEQFLPKAQK
LYLTHIDAEVEGDTHFPDYEPDDWESVFSEFHDADAQNSHSYSFEILERRGSSENRARYKRG
SSAGTGIFAEQTVEVVKSAIETADGALDLYNKYLDQVIPWKTFDETIKELSRFKQEYSQEAS
VLVGDIKVLLMDSQDKYFEATQTVYEWAGVVTQLLSAYIQLFDGYNEKKASAQKDILIRIL
DDGVKKLNEAQKSLLTSSQSFNNASGKLLALDSQLTNDFSEKSSYYQSQVDRIRKEAYAGA
AAGIVAGPFGLIISYSIAAGVIEGKLIPELNNRLKTVQNFFTSLSATVKQANKDIDAAKLKLA
TEIAAIGEIKTETETTRFYVDYDDLMLSLLKGAAKKMINTSNEYRQRHGRKTLFEVPDV*

>DHFR-ClyA (DNA sequence)

ATGGCTCATCATCACCACCACGGTTCAGCTATGATTTCCCTTATTGCAGCACTTGCTG
TTGACCGTGTAATTGGGATGGAGAACGCAATGCCCTGGAACTTGCCCGCCGACCTT
GCATGGTTCAAACGCAACACTTTAGATAAGCCCGTTATCATGGGACGCCACATGTGG
GAGAGCATCGGACGTCCGCTTCCCGGACGCAAAAATATTATTTTGTCGTCGCAACCA
GGGACTGACGACCGTGTAACGTGGGTAAAATCTGTGGATGAAGCAATCGCTGCGGC
GGGCGACGTGCCTGAGATTATGGTAATCGGCGGCGGTCGTGTTTACGAGCAGTTTTT
GCCAAAGGCGCAAAAACTTTACTTAACCCATATCGACGCTGAAGTAGAGGGGGACA
CGCACTTTCCAGACTACGAACCCGACGATTGGGAATCCGTCTTTTCGGAATTTCACG
ACGCCGATGCGCAAAACAGTCATAGTTATTCATTCGAGATTCTTGAGCGTCGCGGCT
CCAGTGAGAAC**CGCGCGCGCTATAAACGC**GGTAGTAGTGCAGGTACGGGTATCTTT
GCGGAACAGACGGTGGAAGTTGTGAAAAGTGCGATTGAAACGGCTGACGGTGCGCT
GGACCTGTATAATAAATATCTGGATCAGGTCATCCCGTGGAAAACCTTTGACGAAAC
GATTAAAGAACTGAGCCGTTTCAAACAGGAATACAGTCAAGAAGCGTCCGTCCTAGT
GGGCGATATCAAAGTGCTGCTGATGGATTCTCAGGACAAATATTTTGAAGCTACCCA
AACGGTTTACGAATGGGCGGGTGTGGTTACCCAGCTGCTGTCCGCATATATTCAGCT
GTTCGATGGATACAATGAGAAAAAAGCGAGCGCGCAGAAAGACATTCTGATCCGCA
TTCTGGATGACGGCGTGAAAAAACTGAATGAAGCCCAGAAATCGCTGCTGACCAGC
TCTCAATCATTTAACAATGCCTCGGGTAAACTGCTGGCACTGGATAGCCAGCTGACG
AACGACTTTTCTGAAAAAAGTTCCTATTACCAGAGCCAAGTCGATCGTATTCGTAAA
GAAGCCTACGCAGGTGCCGCAGCAGGTATTGTGGCCGGTCCGTTCGGTCTGATTATC
TCATATTCAATTGCTGCGGGCGTTATCGAAGGTAAACTGATTCCGGAACTGAACAAT
CGTCTGAAAACCGTTCAGAACTTTTTCACCAGTCTGTCTGCTACGGTCAAACAAGCG
AATAAAGATATCGACGCCGCAAAACTGAAACTGGCCACGGAAATCGCTGCGATTGG
CGAAATCAAAACCGAAACGGAAACCACGCGCTTTTATGTTGATTACGATGACCTGAT
GCTGAGCCTGCTGAAAGGTGCCGCGAAGAAAATGATTAATACCTCTAATGAATATCG
GCAGCGTCACGGTAGAAAAACCCTGTTTGAAGTCCCGGATGTGTAA

>S-FraC-nanobody (protein sequence)

MASADVAGAVIDGAGLGFDVLKTVLEALGNVKRKIAVGIDNESGKTWTAMNTYFRSGT
SDIVLPHKVAHGKALLYNGQKNRGPVATGVVGVIAYSMSDGNTLAVLFSVPYDYNSYSN
WWNVRVYKGQKRADQRMYEELYYHRSPFRGDNGWHSRGLGYGLKSRGFMNSSGHAIL
EIHVTKAGSTQAGSSGSAGSAGQVKLEESGGGSVQTGGSLRLTCAASGRTSRSYGMGWFR
QAPGKEREFVSGISWRGDSTGYADSVKGRFTISRDNAKNTVDLQMNSLKPEDTAIYYCAA
AAGSAWYGTLYEYDYWGQGTQVTVSSGSAGSSHHHHHH*

>S-FraC-nanobody (DNA sequence)

ATGGCGAGCGCCGATGTCGCGGGTGCGGTAATCGACGGTGCGGGTCTGGGCTTTGA
CGTACTGAAAACCGTGCTGGAGGCCCTGGGCAACGTTAAACGCAAAATTGCGGTAG
GGATTGATAACGAATCGGGCAAGACCTGGACAGCGATGAATACCTATTTCCGTTCTG
GTACGAGTGATATTGTGCTCCCACATAAGGTGGCGCATGGTAAGGCGCTGCTGTATAA
CGGTCAAAAAAATCGCGGTCCTGTCGCGACCGGCGTAGTGGGTGTGATTGCCTATAG
TATGTCTGATGGGAACACACTGGCGGTACTGTTCTCCGTGCCGTACGATTATAATAGC
TATAGCAATTGGTGGAACGTGCGTGTCTACAAAGGCCAGAAGCGTGCCGATCAGCGC
ATGTACGAGGAGCTGTACTATCATCGCTCGCCGTTTCGCGGCGACAACGGTTGGCATT
CCCGGGGCTTAGGTTATGGACTCAAAAGTCGCGGCTTTATGAATAGTTCGGGCCACG
CAATCCTGGAGATTCACGTTACCAAAGCAGGCTCAACTCAGGCGGGCAGCTCTGGCT
CTGCTGGTAGCGCTGGGCAGGTAAAGTTAGAAGAAAGCGGTGGGGGATCTGTGCAGA
CCGGCGGTAGCCTGCGCTTGACGTGCGCCGCAAGTGGTCGTACATCTCGCTCATACGG
TATGGGGTGGTTCCGCCAGGCGCCCGGGAAGGAGCGCGAGTTCGTTAGCGGTATCTC
GTGGCGCGGAGACTCAACCGGGTATGCGGATTCTGTAAAAGGCCGTTTCACGATCAG
TCGTGACAACGCAAAAAATACAGTTGACTTGCAGATGAACTCACTGAAACCCGAGGA
TACAGCAATTTATTATTGTGCGGCAGCCGCCGGCTCCGCGTGGTACGGGACGTTATAC
GAATACGACTACTGGGGTCAAGGTACCCAGGTGACCGTATCGAGCGGGTCCGCAGGG
TCGTCCCATCATCACCATCATCACTAATAAGCTT

>DHFR-(TEV)-FraC (protein sequence)

MASAMISLIAALAVDRVIGMENAMPWNLPADLAWFKRNTLDKPVIMGRHTWESIGRPLPG
RKNIILSSQPGTDDRVTVKSVDEAIAAAGDVPEIMVIGGGRVYEQFLPKAQKLYLTHIDAEV
EGDTHFPDYEPDDWESVFSEFHDADAQNSHSYSFEILERRGSS**ENLYFQSK**GSSASADVAGAV
IGGAGLGFDVLKTVLEALGNVKRKIAVGIDNESGKTWTAMNTYFRSGTSDIVLPHKAHGK
ALLYNGQKNRGPVATGVVGVIAYSMSDGNTLAVLFSVPYDYNWYSNWWNVRVYKGQKR
ADQRMYEELYYHRSPFRGDNGWHSRGLGYGLESRGFMNSSGHAILEIHVTKAGSSHHHHH*

>DHFR-(TEV)-FraC (DNA sequence)

CCATGGCTTCAGCTATGATTTCCCTTATTGCAGCACTTGCTGTTGACCGTGTAATTGG
GATGGAGAACGCAATGCCCTGGAACTTGCCCGCCGACCTTGCATGGTTCAAACGCAA
CACTTTAGATAAGCCCGTTATCATGGGACGCCACACGTGGGAGAGCATCGGACGTCCG
CTTCCCGGACGCAAAAATATTATTTTGTCGTCGCAACCAGGGACTGACGACCGTGTAA
CGTGGGTAAAATCTGTGGATGAAGCAATCGCTGCGGCGGGCGACGTGCCTGAGATTA
TGGTAATCGGCGGCGGTCGTGTTTACGAGCAGTTTTTGCCAAAGGCGCAAAAACTTT
ACTTAACCCATATCGACGCTGAAGTAGAGGGGGACACGCACTTTCCAGACTACGAACC
CGACGATTGGGAATCCGTCTTTTCGGAATTTCACGACGCCGATGCGCAAAACAGTCAT
AGTTATTCATTCGAGATTCTTGAGCGTCGCGGCTCCAGT**GAGAACTTATACTTCCAAA**
GTAAGGGTAGTAGTGCAAGTGCTGATGTAGCAGGAGCAGTTATTGGAGGAGCGGGAC
TTGGCTTTGACGTGCTTAAAACTGTTTTAGAAGCGTTAGGCAACGTGAAACGCAAGA
TCGCGGTGGGCATTGACAACGAGAGTGGAAAAACCTGGACCGCTATGAATACTTATT
TTCGTTCGGGGACGAGTGATATCGTGTTGCCGCATAAAGTTGCGCATGGAAAGGCT
TTGCTTTACAACGGGCAAAAAAACCGTGGCCCTGTGGCCACGGGCGTAGTAGGAGT
GATCGCATATTCAATGTCCGATGGTAACACTCTGGCAGTTTTATTCTCCGTTCCTTAT
GATTATAACTGGTATTCAAATTGGTGGAATGTACGTGTGTACAAGGGACAGAAACGC
GCAGATCAACGTATGTATGAGGAACTGTACTACCACCGTTCACCATTTCGTGGTGATA
ACGGGTGGCATTCACGTGGCCTGGGCTACGGATTGGAGAGTCGTGGATTCATGAAC
TCAAGCGGACACGCAATCTTAGAAATTCATGTCACTAAGGCTGGCAGCAGCCATCAT
CACCACCATTAATAAGCTT

>DHFR-(Furin)-FraC-nanobody (protein sequence)

MASAMISLIAALAVDRVIGMENAMPWNLPADLAWFKRNTLDKPVIMGRHTWESIGRPLP
GRKNIILSSQPGTDDRVTWVKSVDEAIAAAGDVPEIMVIGGGRVYEQFLPKAQKLYLTHID
AEVEGDTHFPDYEPDDWESVFSEFHDADAQNSHSYSFEILERRGSSEN**RARYKR**GSSASADV
AGAVIGGAGLGFDVLKTVLEALGNVKRKIAVGIDNESGKTWTAMNTYFRSGTSDIVLPHK
VAHGKALLYNGQKNRGPVATGVVGVIAYSMSDGNTLAVLFSVPYDYNWYSNWWNVRVY
KGQKRADQRMYEELYYHRSPFRGDNGWHSRGLGYGLESRGFMNSSGHAILEIHVTKAGST
RAGSSGSAGSAGQVKLEESGGGSVQTGGSLRLTCAASGRTSRSYGMGWFRQAPGKEREFVS
GISWRGDSTGYADSVKGRFTISRDNAKNTVDLQMNSLKPEDTAIYYCAAAAGSAWYGTLY
EYDYWGQGTQVTVSSGSAGSSHHHHHH*

>DHFR-(Furin)-FraC-nanobody (DNA sequence)

CCATGGCTTCAGCTATGATTTCCCTTATTGCAGCACTTGCTGTTGACCGTGTAATTGG
GATGGAGAACGCAATGCCCTGGAACTTGCCCGCCGACCTTGCATGGTTCAAACGCAA

CACTTTAGATAAGCCCGTTATCATGGGACGCCACACGTGGGAGAGCATCGGACGTCCG
CTTCCCGGACGCAAAAATATTATTTTGTCGTCGCAACCAGGGACTGACGACCGTGTAA
CGTGGGTAAAATCTGTGGATGAAGCAATCGCTGCGGCGGGCGACGTGCCTGAGATTA
TGGTAATCGGCGGCGGTCGTGTTTACGAGCAGTTTTTGCCAAAGGCGCAAAAACTTT
ACTTAACCCATATCGACGCTGAAGTAGAGGGGGACACGCACTTTCCAGACTACGAACC
CGACGATTGGGAATCCGTCTTTTCGGAATTTCACGACGCCGATGCGCAAAACAGTCAT
AGTTATTCATTCGAGATTCTTGAGCGTCGC<u>GGCTCCAGTGAGAAC</u>**<u>CGCGCGCGCTATA</u>**
<u>AACGC</u><u>CGGTAGTAGTGCA</u>AGTGCTGATGTAGCAGGAGCAGTTATTGGAGGAGCGGGAC
TTGGCTTTGACGTGCTTAAAACTGTTTTAGAAGCGTTAGGCAACGTGAAACGCAAGAT
CGCGGTGGGCATTGACAACGAGAGTGGAAAAACCTGGACCGCTATGAATACTTATTTT
CGTTCGGGGACGAGTGATATCGTGTTGCCGCATAAAGTTGCGCATGGAAAGGCTTTG
CTTTACAACGGGCAAAAAAAACCGTGGCCCTGTGGCCACGGGCGTAGTAGGAGTGATC
GCATATTCAATGTCCGATGGTAACACTCTGGCAGTTTTATTCTCCGTTCCTTATGATTA
TAACTGGTATTCAAATTGGTGGAATGTACGTGTGTACAAGGGACAGAAACGCGCAGAT
CAACGTATGTATGAGGAACTGTACTACCACCGTTCACCATTTCGTGGTGATAACGGGT
GGCATTCACGTGGCCTGGGCTACGGATTGGAGAGTCGTGGATTCATGAACTCAAGCG
GACACGCAATCTTAGAAATTCATGTCACTAAGGCT<u>GGCTCAACTCGCGCGGGCAGCTC</u>
<u>TGGCTCTGCTGGTAGCGCTGGG</u>CAGGTAAAGTTAGAAGAAAGCGGTGGGGGATCTGT
GCAGACCGGCGGTAGCCTGCGCTTGACGTGCGCCGCAAGTGGTCGTACATCTCGCTC
ATACGGTATGGGGTGGTTCCGCCAGGCGCCCGGGAAGGAGCGCGAGTTCGTTAGCG
GTATCTCGTGGCGCGGAGACTCAACCGGGTATGCGGATTCTGTAAAAGGCCGTTTCA
CGATCAGTCGTGACAACGCAAAAAATACAGTTGACTTGCAGATGAACTCACTGAAAC
CCGAGGATACAGCAATTTATTATTGTGCGGCAGCCGCCGGCTCCGCGTGGTACGGGA
CGTTATACGAATACGACTACTGGGGTCAAGGTACCCAGGTGACCGTATCGAGCGGGT
CCGCAGGGTCGTCCCATCATCACCATCATCACTAATAAGCTTGG

SUPPORTING INFORMATION

Name of primer	DNA sequence
ClyAXr	TATATATCTCGAGTGCTGCTGCCCACATCCGGGAC
ClyAXf	CACCACTAAAAGCTTGGATCCGGCTGCTAAC
Nbf	ATATATACTCGAGCGGGCTCCTCGGGTTCG
Nbr	TATATATAAGCTTTTATCAGTGGTGATGGTGATGGTGC
5NNN6	GATATAGCCATGGGTACGGGTNNNNNNGCGGAACAGACGGTGGAAG
S272Cf	CTGATGCTGTGCCTGCTGAAAGGTGCCG
S272Cr	CTTTCAGCAGGCACAGCATCAGGTCATCG
DHFRlinkr	TACCTGCACTACTACCGCGTTTATAGCGC
LinkClyA	CCGCGCGCGCTATAAACGCGGTAGTAGTGCAGGTACGGGTATCTTTGCGG AAC
ClyAr	ATATATATAAGCTTACACATCCGGGACTTCAAACAG
W112SFf	ACGATTATAATAGCTATAGCAATTGGTGG
FNlinkr	CAGAGCCAGAGCTGCCCGCCTGAGTTGAGCCAGCCTTAGTGACATGAATTT CTAAG
DFf	ATATCCATGGCTTCAGCTATGATTTCCC
DFr	ATATAAGCTTATTAATGGTGGTGATGATGGC
Furf	GCGTCGCGGCTCCAGTGAGAACCGCGCGCGCTATAAACGCGGTAGTAGTG CAAGTGCTG
DFnHr	AGCCTTAGTGACATGAATTTCTAAG
FraCf	AGTGCTGATGTAGCAGGAGCA
T7-terminator	GCTAGTTATTGCTCAGCGG
T7-promoter	TAATACGACTCACTATAGGG

Table S1. Primers table. N stands for A, G, C or T.

Condition	PCR composition	Cycling conditions
1	Phire Hot Start II DNA polymerase 25 ng template DNA 2 µM of each primer in 50 µL final volume	pre-incubation 98°C for 30 seconds 30 cycles of: denaturation 98 °C for 5 seconds extension 72 °C for 1 minute
2	REDTaq® ReadyMix 100 ng template DNA 2 µM of each primer in 200 µL final volume for 4 reactions	pre-incubation at 95 °C for 3 minutes 30 cycles of: denaturation at 95 °C for 15 seconds annealing at 55 °C for 15 seconds extension at 72°C for 3 minutes
3	Phire Hot Start II DNA polymerase 500 ng template DNA 300 ng primer in 50 µL final volume	pre-incubation 98°C for 30 seconds 30 cycles of: denaturation 98 °C for 5 seconds extension 72 °C for 1.5 minute

Table S2. PCR conditions used for cloning and construction of libraries.

ClyA-nanobody variant	Sequence changes relative to ClyA-nanobody
1	I5C , F6G
SE-ClyA-nanobody	I5S , F6E, R309Q
3	I5A , F6H, Y264C
4	I5S , F6A
5	I5P , F6H
6	I5F , F6R, I251T
7	I5G , F6P, E19G,Q155R
8	I5Q , F6R
9	I5G , F6G

Table S3. Mutations accumulated during directed evolution of ClyA-nanobody gene.

Round	variant	Sequence changes relative to DHFR-TEV-FraC
2	**1**	R318C
2	**2**	S329T, H362L
2	**3**	S139C, S329T, H362L
2	**4**	R102H, R318C
2	**5**	S154N, Y170N
2	**6**	S154N, Y170N, N325D
3	**C-DHFR-FraC**	R318C, **L169R, Y170A, F171R, Q172Y, S173K, K174R**
3	**HC-DHFR-FraC**	R102H, R318C, **L169R, Y170A, F171R, Q172Y, S173K, K174R**
3	**MD-DHFR-FraC**	T50M, N325D, **L169R, Y170A, F171R, Q172Y, S173K, K174R**

Table S4. Mutations accumulated during directed evolution rounds of the DHFR- FraC gene. In bold sequence changes regarding the conversion from TEV to furin cleavage site.

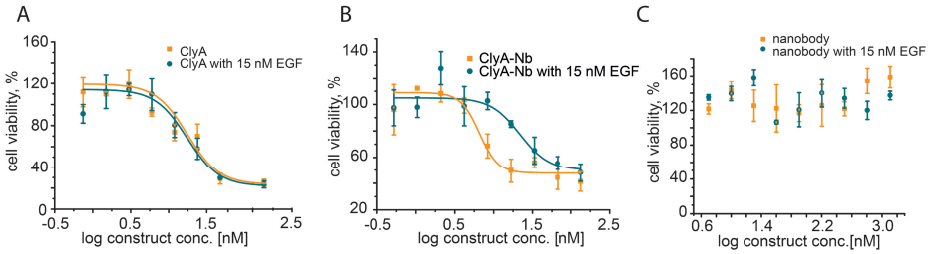

Figure S1. Toxicity of ClyA variants in the presence and absence of 15 nM EGF on A431 epidermoid carcinoma cells. (**A**) ClyA toxicity shows no response on EGF. (**B**) In the presence and absence of 15 nM EGF ClyA-Nb is reduced about two-fold. (**C**) Nanobodies without the toxin have no effect on cell viability.

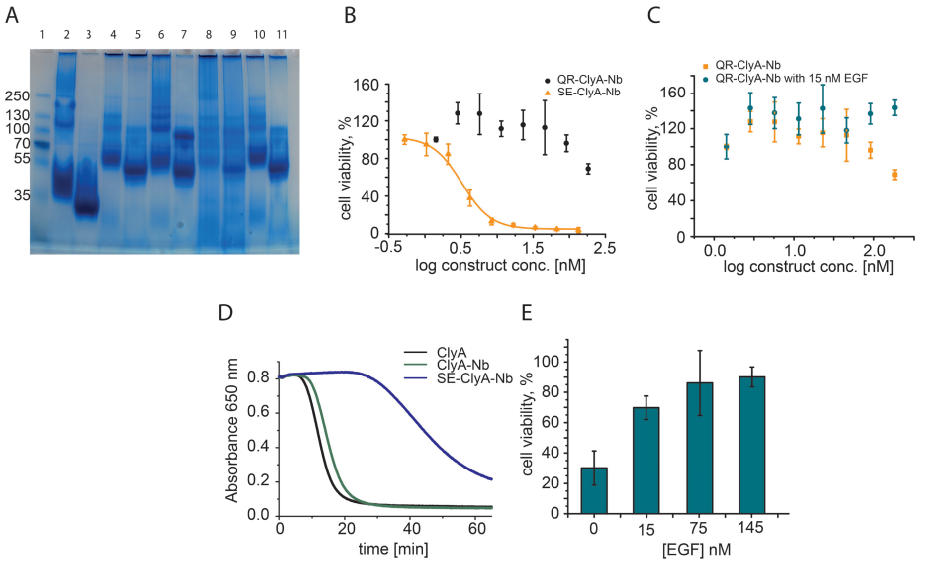

Figure S2. Selection of evolved immunotoxins. (**A**) ClyA-Nb library analyzed by a 4-20% BN-PAGE. Lane 1: Protein ladder, lane 2: ClyA-AS, lane 3: ClyA-AS with 0.2% SDS, lane 4: SA-ClyA-Nb, lane 5: SA-ClyA-Nb with 0.2% SDS, lane 6: KW-ClyA-Nb, lane 7: KW-ClyA-Nb with 0.2% SDS, lane 8: GG-ClyA-Nb, lane 9: GG-ClyA-Nb with 0.2% SDS, lane 10: SV-ClyA-Nb, lane 11: SV-ClyA-Nb with 0.2% SDS. (**B**) Representative dose-response curves of SE-ClyA-Nb and QR-ClyA-Nb on A431 cells. SE mutation increases toxicity, while QR mutation decreases toxicity. (**C**) Representative dose-response curves of QR-ClyA-Nb in the presence and absence of 15 nM EGF. (**D**) Comparison of the hemolytic activity of ClyA and ClyA-Nb constructs. Fusion of ClyA to the Nb extends the time necessary for complete hemolysis of red blood cells, the mutation I5S and F6E of ClyA decreases hemolysis speed even further. (**E**) Comparison of cell viability at 16 nM SE-ClyA-Nb concentrations with increasing EGF concentrations. Cell viability increases up to 90% with increasing EGF concentrations

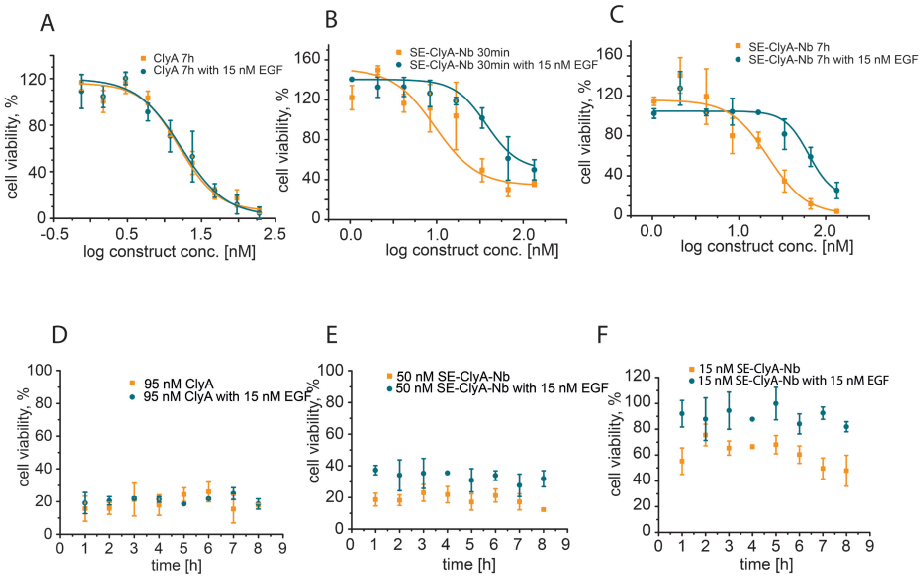

Figure S3. Time and concentration dependence of ClyA cytotoxicity toward A431 cells (**A**) Toxicity of ClyA measured after a 7-hour incubation in the presence and absence of 15 nM EGF. (**B**-**C**) Representative dose-response curves of SE-ClyA-Nb measured after 30 minutes (**B**) or 7 hours (**C**) incubation, before addition and 2 hour incubation of WST-8, in the presence and absence of 15 nM EGF. The addition of EGF reverses the effect of the nanobody and decreases toxicity for the cells. Representative response curves measured after different incubation times using 95 (**D**), 50 (**E**) and 15 (**F**) nM ClyA in the presence and absence of 15 nM EGF. Different incubation times had no effect on the toxicity toward the cells.

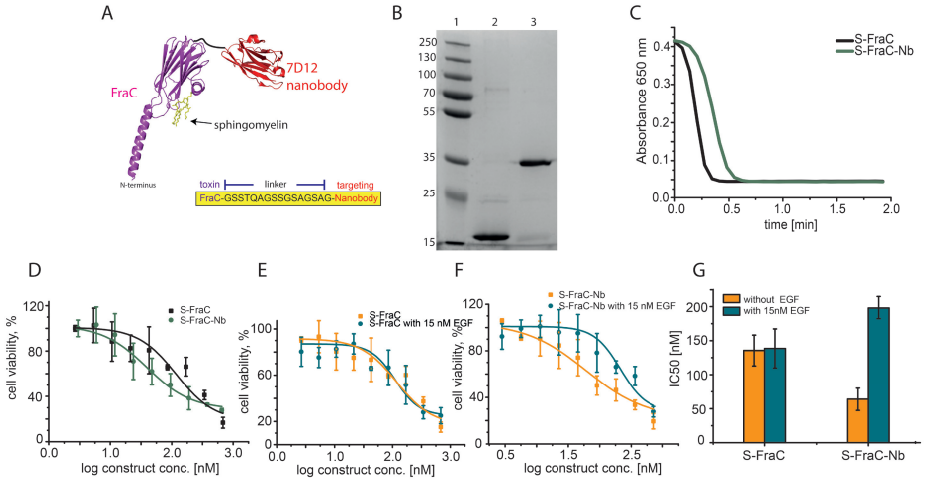

Figure S4. FraC targeting cancer cells. (**A**) Schematic representation of FraC conjugated to nanobody showing FraC (purple, PDB: 4TSY) fused at the C-terminal with the anti-EGFR nanobody 7D12 (red, PDB: 4KRL) spaced by a 16 amino acid long linker (sequence indicated in yellow box). (**B**) S-FraC-nanobody examined by 12% SDS-PAGE. Lane 1: Protein ladder, Lane 2: S-FraC, Lane 3: S-FraC-Nb. (**C**) Comparison of the hemolytic activity of S-FraC and S-FraC-Nb. (**D**) Comparison between the toxicity of S-FraC and S-FraC-Nb for EGFR overexpressing A431 cells. (**E**-**F**) Toxicity of S-FraC and (**E**) S-FraC-Nb (**F**) in the presence and absence of 15 nM EGF. (**G**) Comparison of IC_{50} values of S-FraC and S-FraC-Nb in the presence and absence of EGF.

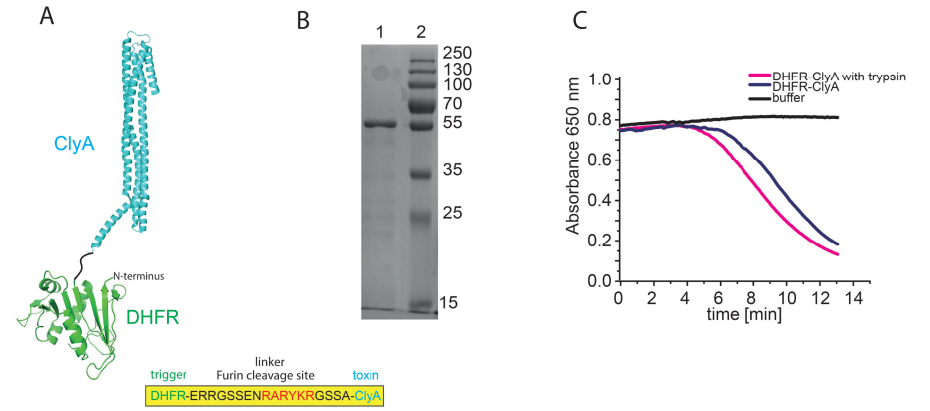

Figure S5. DHFR-ClyA fusion. (**A**) Schematic representation of the conjugate showing ClyA (blue, PDB: 2WCD) fused N-terminal to DHFR (green, PDB: 1RH3) by an 18 amino acid long linker (sequence indicated in yellow box) including a protease cleavage site for furin (indicated in red in yellow box). (**B**) 12% SDS-PAGE gel of the purified DHFR-ClyA chimera examined. Lane 1: DHFR-ClyA, Lane 2: Protein ladder. (**C**) Comparison of the hemolytic activity of DHFR-ClyA and proteolysed DHFR-ClyA. Fusion of ClyA to DHFR did not deactivate the toxin.

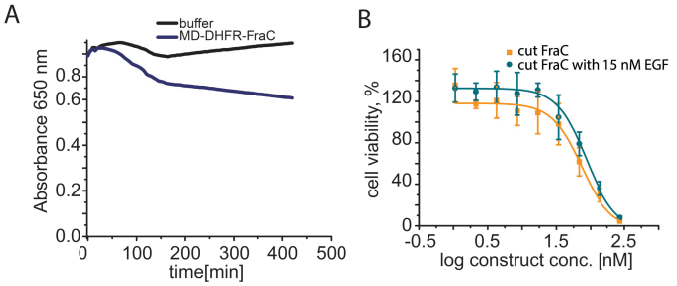

Figure S6. DHFR-FraC fusion. (**A**) Hemolytic activity measurement of MD-DHFR-FraC over 6 hours. No hemolysis of red blood cells could be observed. (**B**) Representative dose-response curves of proteolysed DHFR-FraC in the presence and absence of 15 nM EGF. The addition of EGF had no effect on the toxicity toward the cells.

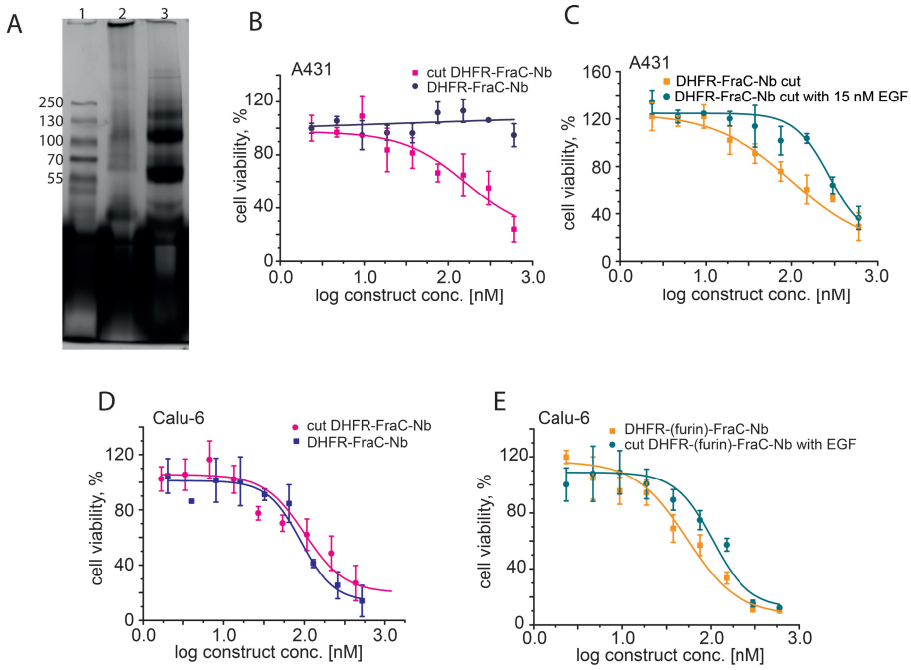

Figure S7. DHFR-FraC fusion. (**A**) DHFR-FraC-Nb analyzed by a 4-20% blue-native PAGE. [40] Lane 1: Protein ladder, lane 2: DHFR-FraC-Nb, lane 3: DHFR-FraC-Nb with 0.2% SDS. Several bands are observed corresponding to monomeric DHFR-FraC-Nb (56 kDa) and, most likely, to multimeric DHFR-FraC-Nb. Interestingly the oligomeric forms of the toxin appear to be SDS stable. FraC is positively charged, hence the faded bands in line 2 (no SDS) are most likely due to protein construct inability of running in native conditions (**B**) Representative dose-response curves of DHFR-FraC-Nb and proteolysed DHFR-FraC-Nb toward A431 cells, showing that only proteolysed DHFR-FraC-Nb is active. (**C**) Representative dose-response curves of proteolysed DHFR-FraC-Nb in the presence and absence of 15 nM EGF tested on A431 cells, showing that the addition of EGF reverses the effect of the nanobody and decreases toxicity for the cells. (**D**) Representative dose-response curves of DHFR-FraC-Nb and proteolysed DHFR-FraC-Nb toward Calu-6 cells, showing that DHFR-FraC-Nb proteolysed by furin expressed by Calu-6 cells gets activated and cause cell death. (**E**) Representative dose-response curves of proteolysed DHFR-FraC-Nb in the presence and absence of 15 nM EGF tested on Calu-6 cells, showing that the addition of EGF reverses the effect of the nanobody and decreases toxicity for the cells.

REFERENCES

(1) Lagassé, H. A. D.; Alexaki, A.; Simhadri, V. L.; Katagiri, N. H.; Jankowski, W.; Sauna, Z. E.; Kimchi-Sarfaty, C. Recent Advances in (Therapeutic Protein) Drug Development. *F1000Research* **2017**, *6*, 113.

(2) Scott, A. M.; Wolchok, J. D.; Old, L. J. Antibody Therapy of Cancer. *Nature Reviews Cancer*. March 22, 2012, pp 278–287.

(3) Samaranayake, H.; Wirth, T.; Schenkwein, D.; Räty, J. K.; Ylä-Herttuala, S. Challenges in Monoclonal Antibody-Based Therapies. *Annals of Medicine*. January 8, 2009, pp 322–331.

(4) Bandaranayake, A. D.; Almo, S. C. Recent Advances in Mammalian Protein Production. *FEBS Lett.* **2014**, *588* (2), 253–260.

(5) Dingermann, T. Recombinant Therapeutic Proteins: Production Platforms and Challenges. *Biotechnol. J.* **2008**, *3* (1), 90–97.

(6) Liu, H. F.; Ma, J.; Winter, C.; Bayer, R. Recovery and Purification Process Development for Monoclonal Antibody Production. *MAbs* **2010**, *2* (5), 480–499.

(7) Minchinton, A. I.; Tannock, I. F. Drug Penetration in Solid Tumours. *Nature Reviews Cancer*. August 2006, pp 583–592.

(8) Rosenberg, A. S.; Sauna, Z. E. Immunogenicity Assessment during the Development of Protein Therapeutics. *J. Pharm. Pharmacol.* **2018**, *70* (5), 584–594.

(9) Baudino, T. Targeted Cancer Therapy: The Next Generation of Cancer Treatment. *Curr. Drug Discov. Technol.* **2015**, *12* (1), 3–20.

(10) Thomas, A.; Teicher, B. A.; Hassan, R. Antibody–drug Conjugates for Cancer Therapy. *Lancet Oncol.* **2016**, *17* (6), e254–e262.

(11) Lambert, J. M.; Berkenblit, A. Antibody-Drug Conjugates for Cancer Treatment. *Annu. Rev. Med.* **2018**, *69* (1), 191–207.

(12) Pastan, I.; Hassan, R.; Fitzgerald, D. J.; Kreitman, R. J. Immunotoxin Therapy of Cancer. *Nat. Rev. Cancer* **2006**, *6* (7), 559–565.

(13) Alewine, C.; Hassan, R.; Pastan, I. Advances in Anticancer Immunotoxin Therapy. *Oncologist* **2015**, *20* (2), 176–185.

(14) Pasche, N.; Neri, D. Immunocytokines: A Novel Class of Potent Armed Antibodies. *Drug Discovery Today*. June 2012, pp 583–590.

(15) Kitson, S. L.; Cuccurullo, V.; Moody, T. S.; Mansi, L. Radionuclide Antibody-Conjugates, a Targeted Therapy towards Cancer. *Curr. Radiopharm.* **2013**, *6* (2), 57–71.

(16) Williams, D. P.; Parker, K.; Bacha, P.; Bishai, W.; Borowski, M.; Genbauffe, F.; Strom, T. B.; Murphy, J. R. Diphtheria Toxin Receptor Binding Domain Substitution with Interleukin-2: Genetic Construction and Properties of a Diphtheria Toxin-Related Interleukin-2 Fusion Protein. *Protein Eng* **1987**, *1* (6), 493–498.

(17) Mansfield, E.; Amlot, P.; Pastan, I.; FitzGerald, D. J. Recombinant RFB4 Immunotoxins Exhibit Potent Cytotoxic Activity for CD22-Bearing Cells and Tumors. *Blood* **1997**, *90* (5), 2020–2026.

(18) Du, X.; Beers, R.; FitzGerald, D. J.; Pastan, I. Differential Cellular Internalization of Anti-CD19 and -CD22 Immunotoxins Results in Different Cytotoxic Activity. *Cancer Res.* **2008**, *68* (15), 6300–6305.

(19) Pirie, C. M.; Hackel, B. J.; Rosenblum, M. G.; Wittrup, K. D. Convergent Potency of Internalized Gelonin Immunotoxins across Varied Cell Lines, Antigens, and Targeting Moieties. *J. Biol. Chem.* **2011**, *286* (6), 4165–4172.

(20) Polito, L.; Mercatelli, D.; Bortolotti, M.; Maiello, S.; Djemil, A.; Battelli, M.; Bolognesi, A. Two Saporin-Containing Immunotoxins Specific for CD20 and CD22 Show Different Behavior in Killing Lymphoma Cells. *Toxins (Basel).* **2017**, *9* (6), 182.

(21) Donaghy, H. Effects of Antibody, Drug and Linker on the Preclinical and Clinical Toxicities of Antibody-Drug Conjugates. *MAbs* **2016**, *8* (4), 659–671.

(22) Srinivasarao, M.; Low, P. S. Ligand-Targeted Drug Delivery. *Chem. Rev.* **2017**, *117* (19), 12133–12164.

(23) Grawunder, U.; Barth, S. *Next Generation Antibody Drug Conjugates (ADCs) and Immunotoxins*; 2017.

(24) Al-Yahyaee, S. A. S.; Ellar, D. J. Cell Targeting of a Pore-Forming Toxin, CytA δ-Endotoxin from Bacillus Thuringiensis Subspecies Israelensis, by Conjugating CytA with Anti-Thy 1 Monoclonal Antibodies and Insulin. *Bioconjug. Chem.* **1996**, *7* (4), 451–460.

(25) Tejuca, M.; Anderluh, G.; Dalla Serra, M. Sea Anemone Cytolysins as Toxic Components of Immunotoxins. *Toxicon* **2009**, *54* (8), 1206–1214.

(26) Wan, L.; Zeng, L.; Chen, L.; Huang, Q.; Li, S.; Lu, Y.; Li, Y.; Cheng, J.; Lu, X. Expression, Purification, and Refolding of a Novel Immunotoxin Containing Humanized Single-Chain Fragment Variable Antibody against CTLA4 and the N-Terminal Fragment of Human Perforin. *Protein Expr. Purif.* **2006**, *48* (2), 307–313.

(27) Avila, A. D.; de Acosta, C. M.; Lage, A. A New Immunotoxin Built by Linking a Hemolytic Toxin to a Monoclonal Antibody Specific for Immature T Lymphocytes. *Int. J. Cancer* **1988**, *42* (4), 568–571.

(28) Avila, A. D.; Mateo Acosta, C. De; Lage, A. A Carcinoembryonic Antigen-Directed Immunotoxin Built by Linking a Monoclonal Antibody to a Hemolytic Toxin. *Int. J. Cancer* **1989**, *43* (5), 926–929.

(29) Avila, A. D.; Calderón, C. F.; Pérez, R. M.; Pons, C.; Pereda, C. M.; Ortiz, A. R. Construction of an Immunotoxin by Linking a Monoclonal Antibody against the Human Epidermal Growth Factor Receptor and a Hemolytic Toxin. *Biol. Res.* **2007**, *40* (2), 173–183.

(30) Tejuca, M.; Díaz, I.; Figueredo, R.; Roque, L.; Pazos, F.; Martínez, D.; Iznaga-Escobar, N.; Pérez, R.; Alvarez, C.; Lanio, M. E. Construction of an Immunotoxin with the Pore Forming Protein StI and Ior C5, a Monoclonal Antibody against a Colon Cancer Cell Line. *Int. Immunopharmacol.* **2004**, *4* (6), 731–744.

(31) Vaidyanathan, M. S.; Sathyanarayana, P.; Maiti, P. K.; Visweswariah, S. S.; Ayappa, K. G. Lysis Dynamics and Membrane Oligomerization Pathways for Cytolysin A (ClyA) Pore-Forming Toxin. *RSC Adv.* **2014**, *4* (10), 4930–4942.

(32) Soletti, R. C.; de Faria, G. P.; Vernal, J.; Terenzi, H.; Anderluh, G.; Borges, H. L.; Moura-Neto, V.; Gabilan, N. H. Potentiation of Anticancer-Drug Cytotoxicity by Sea Anemone Pore-Forming Proteins in Human Glioblastoma Cells. *Anticancer. Drugs* **2008**, *19* (5), 517–525.

(33) Koblinski, J. E.; Ahram, M.; Sloane, B. F. Unraveling the Role of Proteases in Cancer. *Clinica Chimica Acta*. February 15, 2000, pp 113–135.

(34) Jaaks, P.; Bernasconi, M. The Proprotein Convertase Furin in Tumour Progression. *Int. J. Cancer* **2017**, *141* (4), 654–663.

(35) Weldon, J. E.; Skarzynski, M.; Therres, J. A.; Ostovitz, J. R.; Zhou, H.; Kreitman, R. J.; Pastan, I. Designing the Furin-Cleavable Linker in Recombinant Immunotoxins Based on Pseudomonas Exotoxin A. *Bioconjug. Chem.* **2015**, *26* (6), 1120–1128.

(36) Vandooren, J.; Opdenakker, G.; Loadman, P. M.; Edwards, D. R. Proteases in Cancer Drug Delivery. *Adv. Drug Deliv. Rev.* **2016**, *97*, 144–155.

(37) Walker, B.; Bayley, H. A Pore-Forming Protein with a Protease-Activated Trigger. *Protein Eng. Des. Sel.* **1994**, *7* (1), 91–97.

(38) Panchal, R. G.; Cusack, E.; Cheley, S.; Bayley, H. Tumor Protease-Activated, Pore-Forming Toxins from a Combinatorial Library. *Nat. Biotechnol.* **1996**, *14* (7), 852–856.

(39) Mueller, M.; Grauschopf, U.; Maier, T.; Glockshuber, R.; Ban, N. The Structure of a Cytolytic α-Helical Toxin Pore Reveals Its Assembly Mechanism. *Nature* **2009**, *459* (7247), 726–730.

(40) Soskine, M.; Biesemans, A.; De Maeyer, M.; Maglia, G. Tuning the Size and Properties of ClyA Nanopores Assisted by Directed Evolution. *J. Am. Chem. Soc.* **2013**, *135* (36), 13456–13463.

(41) Roovers, R. C.; Vosjan, M. J. W. D.; Laeremans, T.; El Khoulati, R.; De Bruin, R. C. G.; Ferguson, K. M.; Verkleij, A. J.; Van Dongen, G. A. M. S.; Van Bergen En Henegouwen, P. M. P. A Biparatopic Anti-EGFR Nanobody Efficiently Inhibits Solid Tumour Growth. *Int. J. Cancer* **2011**, *129* (8), 2013–2024.

(42) Roovers, R. C.; Laeremans, T.; Huang, L.; De Taeye, S.; Verkleij, A. J.; Revets, H.; De Haard, H. J.; Van Bergen En Henegouwen, P. M. P. Efficient Inhibition of EGFR Signalling and of Tumour Growth by Antagonistic Anti-EGFR Nanobodies. *Cancer Immunol. Immunother.* **2007**, *56* (3), 303–317.

(43) Umekita, Y.; Ohi, Y.; Sagara, Y.; Yoshida, H. Co-Expression of Epidermal Growth Factor Receptor and Transforming Growth Factor-α Predicts Worse Prognosis in Breast-Cancer Patients. *Int. J. Cancer* **2000**, *89* (6), 484–487.

(44) Nicholson, R. I.; Gee, J. M.; Harper, M. E. EGFR and Cancer Prognosis. *Eur. J. Cancer* **2001**, *37 Suppl 4*, S9-15.

(45) Ullrich, A.; Coussens, L.; Hayflick, J. S.; Dull, T. J.; Gray, A.; Tam, A. W.; Lee, J.; Yarden, Y.; Libermann, T. A.; Schlessinger, J. Human Epidermal Growth Factor Receptor CDNA Sequence and Aberrant Expression of the Amplified Gene in A431 Epidermoid Carcinoma Cells. *Nature 309* (5967), 418–425.

(46) Tanaka, K.; Caaveiro, J. M. M.; Morante, K.; González-Manãs, J. M.; Tsumoto, K. Structural Basis for Self-Assembly of a Cytolytic Pore Lined by Protein and Lipid. *Nat. Commun.* **2015**, *6*, 6337.

(47) Mbikay, M.; Sirois, F.; Yao, J.; Seidah, N. G.; Chrétien, M. Comparative Analysis of Expression of the Proprotein Convertases Furin, PACE4, PC1 and PC2 in Human Lung Tumours. *Br. J. Cancer* **1997**, *75* (10), 1509–1514.

(48) Siegfried, G.; Basak, A.; Cromlish, J. A.; Benjannet, S.; Marcinkiewicz, J.; Chrétien, M.; Seidah, N. G.; Khatib, A. M. The Secretory Proprotein Convertases Furin, PC5, and PC7 Activate VEGF-C to Induce Tumorigenesis. *J. Clin. Invest.* **2003**, *111* (11), 1723–1732.

(49) Mazar, A. P.; Henkin, J.; Goldfarb, R. H. The Urokinase Plasminogen Activator System in Cancer: Implications for Tumor Angiogenesis and Metastasis. *Angiogenesis* **1999**, *3* (1), 15–32.

(50) Mohamed, M. M.; Sloane, B. F. Cysteine Cathepsins: Multifunctional Enzymes in Cancer. In *Nature Reviews Cancer*; 2006; Vol. 6, pp 764–775.

(51) Bassi, D. E.; Mahloogi, H.; Al-Saleem, L.; De Cicco, R. L.; Ridge, J. A.; Klein-Szanto, A. J. P. Elevated Furin Expression in Aggressive Human Head and Neck Tumors and Tumor Cell Lines. *Mol. Carcinog.* **2001**, *31* (4), 224–232.

(52) Bassi, D. E.; Zhang, J.; Renner, C.; Klein-Szanto, A. J. Targeting Proprotein Convertases in Furin-Rich Lung Cancer Cells Results in Decreased in Vitro and in Vivo Growth. *Mol. Carcinog.* **2017**, *56* (3), 1182–1188.

(53) Schaeybroeck, S. V. Chemotherapy-Induced Epidermal Growth Factor Receptor Activation Determines Response to Combined Gefitinib/Chemotherapy Treatment in Non-Small Cell Lung Cancer Cells. *Mol. Cancer Ther.* **2006**, *5* (5), 1154–1165.

(54) Van Der Linden, R. H. J.; Frenken, L. G. J.; De Geus, B.; Harmsen, M. M.; Ruuls, R. C.; Stok, W.; De Ron, L.; Wilson, S.; Davis, P.; Verrips, C. T. Comparison of Physical Chemical Properties of Llama V(HH) Antibody Fragments and Mouse Monoclonal Antibodies. *Biochim. Biophys. Acta - Protein Struct. Mol. Enzymol.* **1999**, *1431* (1), 37–46.

(55) Bannas, P.; Well, L.; Lenz, A.; Rissiek, B.; Haag, F.; Schmid, J.; Hochgräfe, K.; Trepel, M.; Adam, G.; Ittrich, H.; et al. In Vivo Near-Infrared Fluorescence Targeting of T Cells: Comparison of Nanobodies and Conventional Monoclonal Antibodies. *Contrast Media Mol. Imaging* **2014**, *9* (2), 135–142.

(56) Cortez-Retamozo, V.; Lauwereys, M.; Hassanzadeh Gh., G.; Gobert, M.; Conrath, K.; Muyldermans, S.; De Baetselier, P.; Revets, H. Efficient Tumor Targeting by Single-Domain Antibody Fragments of Camels. *Int. J. Cancer* **2002**, *98* (3), 456–462.

(57) Thomas, G. Furin at the Cutting Edge: From Protein Traffic to Embryogenesis and Disease. *Nature Reviews Molecular Cell Biology*. October 2002, pp 753–766.

(58) Kim, J. Y.; Doody, A. M.; Chen, D. J.; Cremona, G. H.; Shuler, M. L.; Putnam, D.; DeLisa, M. P. Engineered Bacterial Outer Membrane Vesicles with Enhanced Functionality. *J. Mol. Biol.* **2008**, *380* (1), 51–66.

(59) Miles, G.; Cheley, S.; Braha, O.; Bayley, H. The Staphylococcal Leukocidin Bicomponent Toxin Forms Large Ionic Channels. *Biochemistry* **2001**, *40* (29), 8514–8522.

(60) Miyazaki, K. MEGAWHOP Cloning: A Method of Creating Random Mutagenesis Libraries via Megaprimer PCR of Whole Plasmids. *Methods Enzymol.* **2011**, *498*, 399–406.

(61) Wloka, C.; Mutter, N. L.; Soskine, M.; Maglia, G. Alpha-Helical Fragaceatoxin C Nanopore Engineered for Double-Stranded and Single-Stranded Nucleic Acid Analysis. *Angew. Chem. Int. Ed. Engl.* **2016**, *55* (40), 12494–12498.

(62) Sawaya, M. R.; Kraut, J. Loop and Subdomain Movements in the Mechanism of Escherichia Coli Dihydrofolate Reductase: Crystallographic Evidence. *Biochemistry* **1997**, *36* (3), 586–603.

(63) Wilson, D. S.; Keefe, A. D. Random Mutagenesis by PCR. In *Current Protocols in Molecular Biology*; John Wiley & Sons, Inc.: Hoboken, NJ, USA, 2001; Vol. Chapter 8, Unit8.3.